

## ■ Noncovalent Interactions

# 5-Aza-7-deazaguanine–Isoguanine and Guanine–Isoguanine Base Pairs in Watson–Crick DNA: The Impact of Purine Tracts, Clickable Dendritic Side Chains, and Pyrene Adducts

Aigui Zhang,<sup>[a]</sup> Dasharath Kondhare,<sup>[a]</sup> Peter Leonard,<sup>[a]</sup> and Frank Seela<sup>\*,[a, b]</sup>

**Abstract:** The Watson–Crick coding system depends on the molecular recognition of complementary purine and pyrimidine bases. Now, the construction of hybrid DNAs with Watson–Crick and purine–purine base pairs decorated with dendritic side chains was performed. Oligonucleotides with single and multiple incorporations of 5-aza-7-deaza-2'-deoxyguanosine, its tripropargylamine derivative, and 2'-deoxyisoguanosine were synthesized. Duplex stability decreased if single modified purine–purine base pairs were inserted, but increased if pyrene residues were introduced by click chemistry. A growing number of consecutive 5-aza-7-deaza-

guanine–isoguanine base pairs led to strong stepwise duplex stabilization, a phenomenon not observed for the guanine–isoguanine base pair. Spacious residues are well accommodated in the large groove of purine–purine DNA tracts. Changes to the global helical structure monitored by circular dichroism spectroscopy show the impact of functionalization to the global double-helix structure. This study explores new areas of molecular recognition realized by purine base pairs that are complementary in hydrogen bonding, but not in size, relative to canonical pairs.

## Introduction

The DNA coding system relies on the molecular recognition of complementary purine and pyrimidine bases. Complementary hydrogen bonds between donor and acceptor atoms of nucleobases connect DNA single strands and form bidentate dA–dT and tridentate dG–dC base pairs of complementary size. The so-formed DNA double helix displays antiparallel chain orientation and + helicity.<sup>[1]</sup> An alternative purine–purine base pairing system with a guanine–isoguanine pair in a Watson–Crick double helix was reported in 1999 by our laboratory (Figure 1c, motif I).<sup>[2]</sup> Earlier, this tridentate base pair was identified in pyranose DNA by Eschenmoser et al.<sup>[3]</sup> Later, the guanine–


isoguanine base pair was incorporated in all-purine DNA.<sup>[4]</sup> Size-extended base pairs were also constructed by the group of Kool based on nucleosides reported by the group of Leonard.<sup>[5]</sup>


The presence of two complementary purines in a base pair enlarges the size of the double helix and the distance between the anomeric centers. As a result, the purine–purine base pairs break the principle of Watson–Crick size complementarity, but can retain the Watson–Crick hydrogen-bonding pattern.<sup>[6]</sup> Helix distortion occurs if the purine–purine helix is embedded in a Watson–Crick helix. Changes in helix diameter can cause destabilization near the connection points.<sup>[6]</sup>

In 2001, we reported on a pairing system formed by 5-aza-7-deazaguanine and isoguanine (Figure 1c, motif II).<sup>[7]</sup> 5-Aza-7-deaza-2'-deoxyguanosine (**1**) represents a 2'-deoxyguanosine analogue with the recognition face of the pyrimidine nucleoside 2'-deoxyisocytidine. Nucleoside **1** was synthesized and incorporated into DNA.<sup>[8]</sup> The shift of nitrogen-7 to bridgehead position-5 makes nitrogen-1 an acceptor site and not a donor as in guanine. Consequently, 5-aza-7-deazaguanine forms a base pair with isoguanine to give purine–purine DNA with the common antiparallel-chain orientation and with guanine to form DNA with a parallel-chain alignment.<sup>[6a,7,9]</sup> Contrary to the guanine–isoguanine base pair, the tautomeric shift for the formation of a tridentate 5-aza-7-deazaguanine–isoguanine pair is not necessary. Later, base pairs of xanthine or 7-deazaxanthine with 2,6-diaminopurine or a 2,6-diaminopurine analogue were described.<sup>[4b,10]</sup> Recently, DNA with 5-aza-7-deazaguanine–isoguanine pairs was characterized by X-ray analysis.<sup>[6a]</sup> According to the solid-state structure, complementary purine bases form hydrogen bonds in a similar way to that of complementary pu-

[a] Dr. A. Zhang, Dr. D. Kondhare, Dr. P. Leonard, Prof. Dr. F. Seela  
Laboratory of Bioorganic Chemistry and Chemical Biology  
Center for Nanotechnology, University of Münster  
Heisenbergstrasse 11  
48149 Münster (Germany)

[b] Prof. Dr. F. Seela  
Laboratorium für Organische und Bioorganische Chemie  
Institut für Chemie neuer Materialien, Universität Osnabrück  
Barbarastrasse 7, 49069 Osnabrück (Germany)  
E-mail: Frank.Seela@uni-osnabrueck.de  
Homepage: www.seela.net

 Supporting information and the ORCID identification number(s) for the author(s) of this article can be found under:  
<https://doi.org/10.1002/chem.202005199>

 © 2021 The Authors. Chemistry - A European Journal published by Wiley-VCH GmbH. This is an open access article under the terms of the Creative Commons Attribution Non-Commercial NoDerivs License, which permits use and distribution in any medium, provided the original work is properly cited, the use is non-commercial and no modifications or adaptations are made.

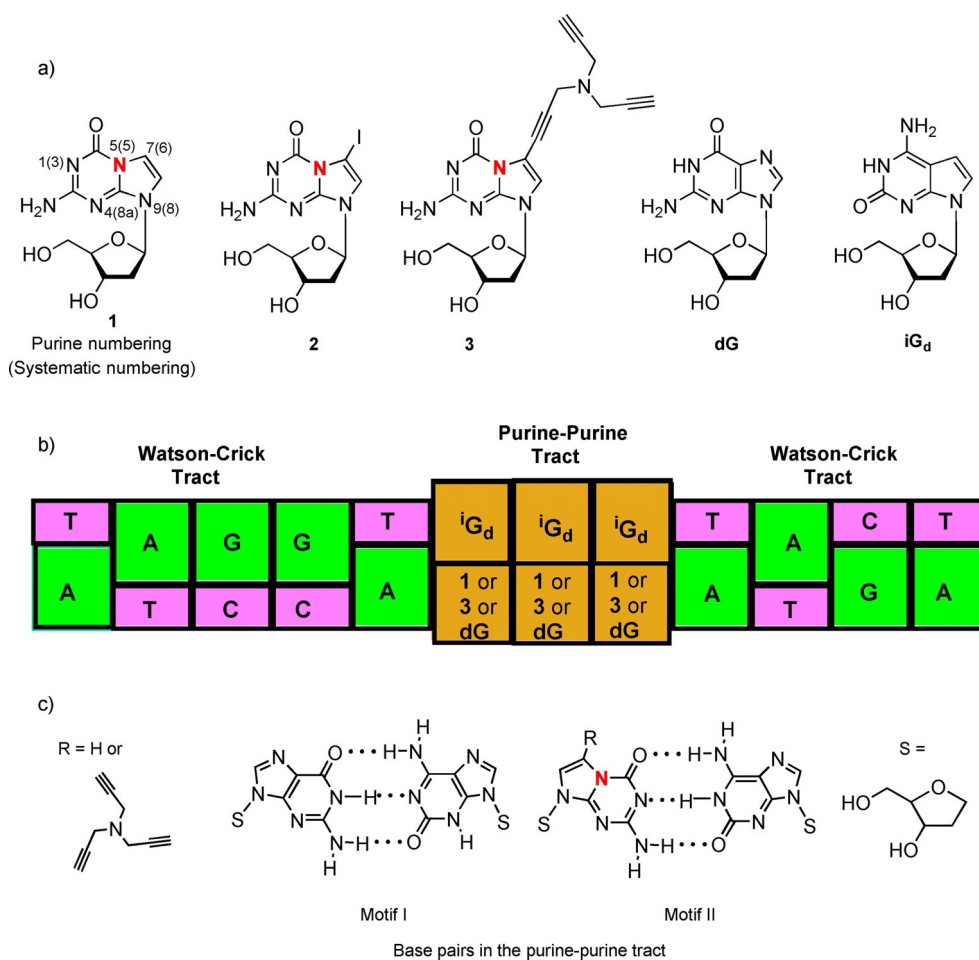


**Figure 1.** a) Structures of nucleosides used in this study. iG<sub>d</sub> corresponds to 2'-deoxyisoguanosine. dG corresponds to 2'-deoxyguanosine. b) Schematic view of a double helix containing purine-purine base pairs bearing clickable side chains in the core of a Watson-Crick double helix. c) Proposed base pairs. T, A, G, and C correspond to 2'-deoxythymidine, 2'-deoxyadenosine, 2'-deoxyguanosine, and 2'-deoxycytidine, respectively.

riines with pyrimidines. Most of the existing work has been reviewed.<sup>[9]</sup>

Until now, nothing has been known about functionalized 5-aza-7-deazaguanine-isoguanine base pairs in DNA. This inspired us to functionalize the 5-aza-7-deazaguanine-isoguanine base pair by introducing side chains at position-7 of the 5-aza-7-deazaguanine base (Figure 1 a). Recently, the introduction of various side chains to nucleoside **1** was reported.<sup>[11]</sup> From this, we choose clickable tripropargylamine side-chain derivative **3** to study its impact on DNA stability and helix structure. The dendritic (branched) side chain contains two terminal triple bonds, which can be functionalized by click chemistry.<sup>[12]</sup> Dendronized oligonucleotides find application as signal amplifiers in nucleic acid quantification for the detection of viral infections,<sup>[13]</sup> for drug delivery, in nanomedicine, and for nanoscale electronics.<sup>[14]</sup> Multifunctionalized DNA probes have been employed to amplify fluorescence signals in hybridization studies.<sup>[15]</sup> Nonetheless, the dendronized 5-aza-7-deazaguanine-isoguanine base pair represents the first example of a nucleobase-functionalized purine-purine pair in DNA. Here, the term purine-purine base pair stands for canonical purine pairs and those with modified purine skeletons.

To access oligonucleotides incorporating dendronized 5-aza-7-deazaguanine nucleoside **3**, the nucleoside was converted into a phosphoramidite and applied to solid-phase oligonucleotide synthesis. Single, as well as double and triple, incorporations into oligonucleotides were performed. The modified oligonucleotides were used to construct hybrid DNA duplexes consisting of functionalized purine-purine DNA base pairs flanked by Watson-Crick pairs (Figure 1 b,c). For comparison, the corresponding duplex constructs with guanine-isoguanine pairs and nonfunctionalized **1** were prepared and investigated. Melting experiments were performed and  $T_m$  values, as well as thermodynamic data, were determined to characterize duplex stability. Circular dichroism (CD) spectroscopy was used to detect global changes to the helix structure. Pyrene azide was chosen for the double click reaction because pyrene residues can stabilize DNA by intercalation and display monomer and excimer fluorescence.<sup>[16]</sup>

## Results and Discussion

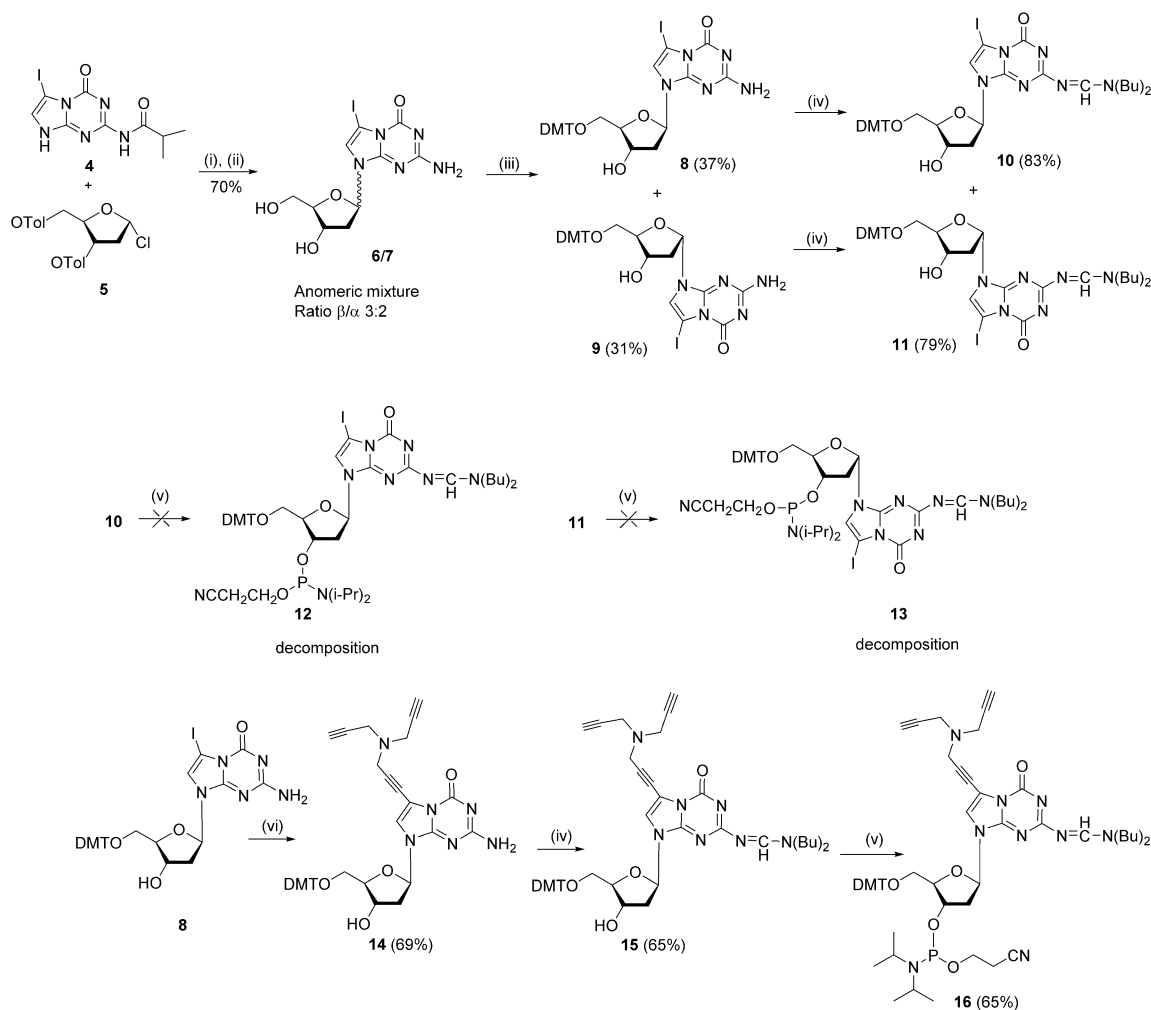
### Synthesis and characterization of 5-aza-7-deaza-2'-deoxyguanosine building blocks with 7-triopropargylamine side chains

The syntheses of 7-triopropargylamino derivative **3**, its  $\alpha$ -D anomer, and its 5-aza-7-deaza-7-iodo-2'-deoxyguanosine precursor (**2**) have been reported.<sup>[11]</sup> However, the protocol to access **2** was laborious because the glycosylation of isobutyrylated 5-aza-7-deaza-7-iodoguanine **4** with the Hoffer sugar resulted in a mixture of  $\alpha$ -D and  $\beta$ -D anomers ( $\beta/\alpha = 3:2$ ). They were separated by a combination of recrystallization and chromatography. Direct purification was not possible due to the identical chromatographic mobility of the anomers. Afterwards, Sonogashira cross-coupling reactions were performed to introduce various side chains.<sup>[11b,c]</sup> Now, the separation of anomers was improved. For this, nucleobase anion glycosylation and deprotection was performed in one step (70% yield) and the crude mixture was directly converted into a mixture of  $\alpha/\beta$ -D

DMT derivatives **8/9** (Scheme 1). The anomers could be separated by column chromatography, affording  $\beta$ -D anomer **8** in 37% yield and  $\alpha$ -D anomer **9** in 31% yield. For the synthesis of phosphoramidite building blocks, compounds **8** and **9** were protected at the 2-amino group with dibutylformamide dimethyl acetal, yielding amino-protected nucleosides **10** ( $\beta$ -D) and **11** ( $\alpha$ -D) in 83 and 79% yield, respectively.

However, phosphorylation performed on **10** or **11** failed and led to complete decomposition of the starting materials within 5 min (Scheme 1; for details, see the Experimental Section). Thus, iodo nucleosides **6** and **7** could not be used for oligonucleotide synthesis and functionalization.

Consequently, another route was chosen. For this study, only the phosphoramidite of the  $\beta$ -D-anomer was required; thus, we focused our synthetic efforts on this compound. Therefore, DMT-protected nucleoside **8** was used as a starting material for the Sonogashira reaction to obtain tripropargylamine side-chain derivative **14** in 69% yield (Scheme 1). Then, the 2-amino group was protected with a dibutylamidine residue, forming **15** in 65%.



**Scheme 1.** Synthesis of anomeric 7-iodinated 5-aza-7-deazaguanine 2'-deoxyribose nucleoside 4,4'-dimethoxytrityl (DMT) derivatives and dendronized phosphoramidite **16**. Reagents and conditions: i) tris[2-(2-methoxyethoxy)ethyl]amine (TDA-1),  $K_2CO_3$ , MeCN, RT, 1.5 h; ii)  $NH_3/MeOH$ , RT, overnight; iii) DMT-Cl, pyridine, RT, 3 h; iv)  $Bu_2NCH(OMe)_2$ , MeOH, 40 °C, 4 h; v)  $NC(OCH_2)_2P(O)(Cl)N(iPr)_2$ ,  $(iPr)_2NEt$ , RT; vi) CuI,  $[Pd(PPh_3)_4]$ , triethylamine, tripropargylamine, RT. Tol: tolyl.

In this case, phosphoramidite synthesis with 2-cyanoethyl diisopropylphosphoramido chloridite worked smoothly and compound **16** was isolated in 65% yield as a mixture of *Rp/Sp* diastereoisomers. Other modified phosphoramidites used in this study (for structures, see Figure S1 in the Supporting Information) were prepared as described in the literature.<sup>[7,17]</sup> All newly synthesized compounds were characterized by <sup>1</sup>H and <sup>13</sup>C NMR spectroscopy, as well as ESI-TOF MS (see the Experimental Section). The <sup>1</sup>H–<sup>13</sup>C correlated (HMBC and HSQC) NMR spectra were used to assign the <sup>13</sup>C NMR signals. For details, see the Experimental Section (for spectra, see the Supporting Information).

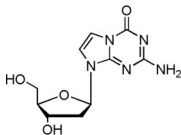
### Oligonucleotide synthesis and characterization

For purine–purine base pairing studies, a series of oligonucleotides (ODNs) containing **1**, tripropargylamino derivative **3**, dG,

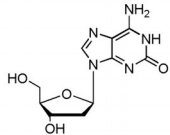
and 2'-deoxyisoguanosine (<sup>i</sup>G<sub>d</sub>) were synthesized. To this end, automated solid-phase synthesis was performed and the modified phosphoramidites of **1**,<sup>[7]</sup> **3**, and <sup>i</sup>G<sub>d</sub><sup>[17]</sup> (for structures, see the Supporting Information) were used together with standard building blocks. The coupling yields of the modified building blocks were always higher than 95%. Single and multiple incorporations of the modified nucleosides were performed. After synthesis, oligonucleotides were cleaved from the solid support and deprotected in concentrated 28% aqueous ammonia at 55 °C for 2 h and then at RT overnight. Detritylation was performed with 2.5% dichloroacetic acid in CH<sub>2</sub>Cl<sub>2</sub>. Oligonucleotides were purified before and after detritylation by means of reversed-phase HPLC on an RP-18 column. HPLC purity profiles are documented in the Supporting Information (Figure S3). Subsequently, molecular masses were determined by MALDI-TOF MS. Table 1 displays the oligonucleotide sequences and their masses.

**Table 1.** Synthesized oligonucleotides and their molecular masses determined by means of MALDI-TOF MS.

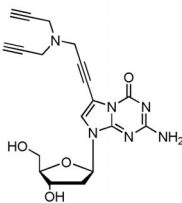
Oligonucleotide	Calcd <sup>[a]</sup>	Molecular weight	
		Expt <sup>[b]</sup>	
ODN-1	5'-d (TAGGTCAACT)	–	–
ODN-2	5'-d (AGTATTGACCTA)	–	–
ODN-3	5'-d (TAG <sup>1</sup> GTCAACT)	3644.4	3644.0
ODN-4	5'-d (AGTATTGAGCTA) <sup>[c]</sup>	3684.5	3684.0
ODN-5	5'-d (AGTATTGA <sup>1</sup> GCTA)	3684.5	3684.4
ODN-6	5'-d (AGTATTGA <sup>1</sup> CTA) <sup>[c]</sup>	3684.5	3684.0
ODN-7	5'-d (AGT ATT GA <sup>3</sup> CTA) <sup>[c]</sup>	3813.6	3813.0
ODN-8	5'-d (TA <sup>1</sup> G <sup>1</sup> GTCAACT) <sup>[7]</sup>	3645.4	3644.9
ODN-9	5'-d (AGTATTGAGGTA)	3724.5	3724.9
ODN-10	5'-d (AGTATTGA <sup>11</sup> TA) <sup>[c]</sup>	3724.4	3724.0
ODN-11	5'-d (AGTATTGA <sup>33</sup> TA) <sup>[c]</sup>	3982.8	3982.0
ODN-12	5'-d (TAGGT <sup>1</sup> GAATA <sup>1</sup> GT)	3724.5	3725.3
ODN-13	5'-d (A <sup>1</sup> TATT <sup>1</sup> ACCTA) <sup>[9a]</sup>	3645.2	3646.3
ODN-14	5'-d (A <sup>3</sup> TATT <sup>3</sup> ACCTA) <sup>[c]</sup>	3902.8	3902.0
ODN-15	5'-d (TAGGT <sup>1</sup> G <sup>1</sup> G <sup>1</sup> GTA)	3716.5	3716.2
ODN-16	5'-d (TAGGTGGGTACT)	3716.5	3717.0
ODN-17	5'-d (AGTAGGGACCTA)	3694.5	3695.0
ODN-18	5'-d (AGTA <sup>111</sup> ACCTA)	3694.5	3694.3
ODN-19	5'-d (AGTA <sup>333</sup> ACCTA)	4082.0	4082.4
ODN-20	5'-d (AGTACCCACCTA)	3574.4	3575.3
ODN-21	5'-d (AGTATTGA <sup>18</sup> CTA)	4328.2	4330.2



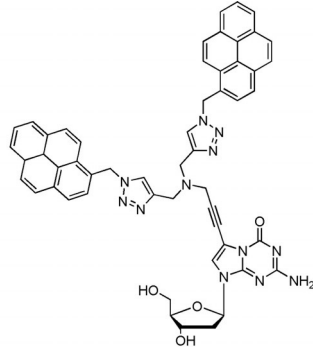
**1**



<sup>i</sup>G<sub>d</sub>



**3**



**18**

[a] Calculated on the basis of the molecular mass  $[M+H]^+$ . [b] Determined by means of MALDI-TOF MS in linear positive mode. [c] Determined by means of MALDI-TOF MS in linear negative mode. **1** corresponds to 5-aza-7-deaza-2'-deoxyguanosine. **3** corresponds to 7-tripropargylamine-5-aza-7-deaza-2'-deoxyguanosine. <sup>i</sup>G<sub>d</sub> corresponds to 2'-deoxyisoguanosine. **18** corresponds to bis-pyrene click adduct of 7-tripropargylamine-5-aza-7-deaza-2'-deoxyguanosine

## 5-Aza-7-deazaguanine–isoguanine and guanine–isoguanine base-pair stability

According to our experience on the impact of tripropargylamine residues on Watson–Crick base pairs,<sup>[12d,e,16f,g,II]</sup> we anticipated that this side chain might have a stabilizing effect on 5-aza-7-deazaguanine base pairs in purine–purine tracts. Also, additional residues introduced by click chemistry might stabilize DNA further. To this end, the impact of tripropargylamine side chains on the stability of the 5-aza-7-deazaguanine base pairs and the click functionalization of terminal triple bonds were studied; this represents the first example of the functionalization of a purine–purine pair formed by a 5-aza-7-deazaguanine–isoguanosine pair.

More specifically, Watson–Crick base pairs of the duplex ODN-1•ODN-2 were replaced stepwise by the incorporation of an increasing number of purine–purine base pairs. In the first set of experiments, oligonucleotides with single incorporations of **1**, **3**, and dG at identical positions were hybridized with complementary strands containing <sup>i</sup>G<sub>d</sub> opposite to the modified residues. This afforded duplexes with dG–<sup>i</sup>G<sub>d</sub>, **1**–<sup>i</sup>G<sub>d</sub>, and **3**–<sup>i</sup>G<sub>d</sub> base pairs. Then, melting experiments were performed in 0.1 M NaCl, 0.01 M MgCl<sub>2</sub>, and 0.01 M Na-cacodylate. Melting profiles of duplexes with one to three purine base-pair incorporations are depicted in Figure 2. All curves displayed cooperative melting. From the curves, it is evident that 1) the duplex stability decreases if a single purine–purine base pair is incorporated, 2) duplex stability increases if an increasing number of 5-aza-7-deazaguanine–isoguanine base pairs are present, and 3) stabilization is particularly strong if tripropargylamine side chains are introduced. On the contrary, duplexes with dG–<sup>i</sup>G<sub>d</sub> base pairs showed low *T<sub>m</sub>* values and no positive change upon increasing the number of base pairs. The stability of duplexes with multiple incorporations increased in the following order: dG–<sup>i</sup>G<sub>d</sub> < **1**–<sup>i</sup>G<sub>d</sub> < **3**–<sup>i</sup>G<sub>d</sub>.

*T<sub>m</sub>* values and thermodynamic data of all melting curves are summarized in Tables 2 and 3. Thermodynamic data were calculated by shape analysis of the melting curves. Table 2 displays *T<sub>m</sub>* values for duplexes incorporating single purine–purine base pair combinations. Data clearly indicate that all single base-pair replacements act as mismatches. Also, combinations that should form base pairs (Table 2, upper part) form duplexes less stable than the Watson–Crick duplex ODN-1•ODN-2. Apparently, the free energy loss by local switches from a purine–purine pair to proximal purine–pyrimidine pairs is the reason. The lower part of Table 2 shows purine–purine mismatches. In this case, the *T<sub>m</sub>* values are even lower. However, from these data (upper vs. lower part of Table 2), the capability of guanine–isoguanine and 5-aza-7-deazaguanine–isoguanine base-pair formation is visible.

Table 3 displays data for two and three incorporations of purine–purine base pairs. *T<sub>m</sub>* data show that multiple consecutive base pairs (two or three) of **1** or **3** with <sup>i</sup>G<sub>d</sub> increase duplex stability substantially compared with single incorporations. Now, the *T<sub>m</sub>* values are equal (2 incorporations) or higher (3 incorporations) than those for the standard Watson–Crick duplex. Moreover, consecutive dendronized **3**–<sup>i</sup>G<sub>d</sub> base pairs

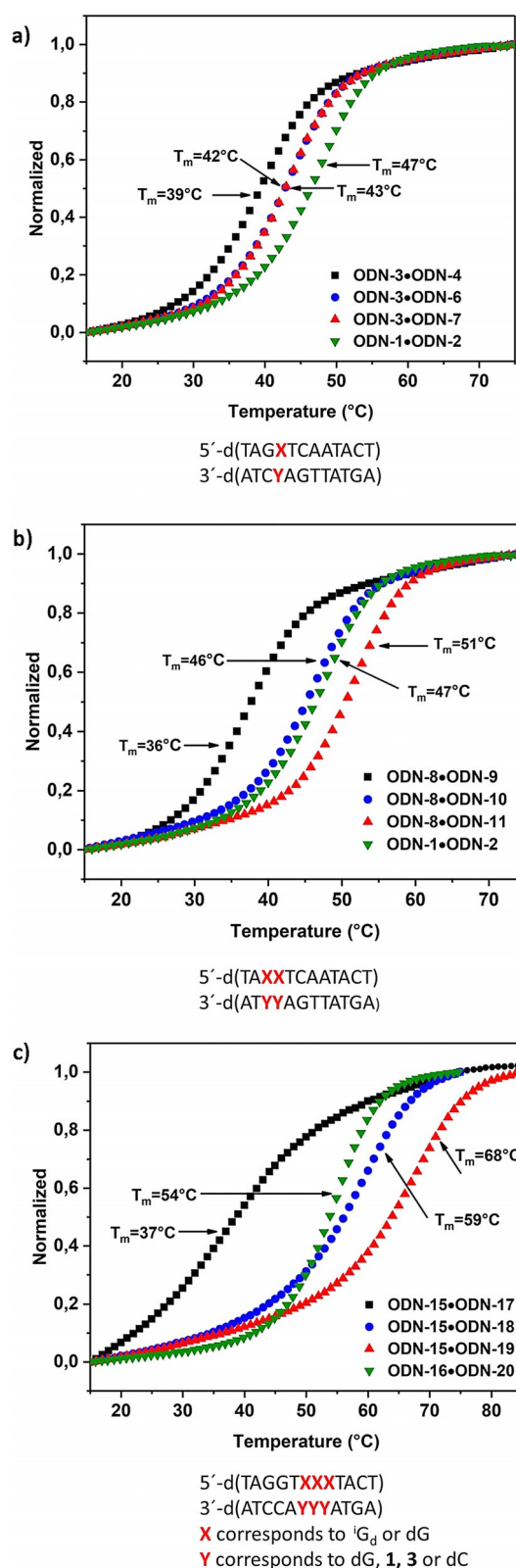


**Figure 2.** Thermal denaturation experiments of duplexes a) ODN-3•ODN-4 (black), ODN-3•ODN-6 (blue), ODN-3•ODN-7 (red), and ODN-1•ODN-2 (green); b) ODN-8•ODN-9 (black), ODN-8•ODN-10 (blue), ODN-8•ODN-11 (red), and ODN-1•ODN-2 (green); and c) ODN-15•ODN-17 (black), ODN-15•ODN-18 (blue), ODN-15•ODN-19 (red), and ODN-16•ODN-20 (green). All measurements were performed with 5 μM + 5 μM single-strand concentrations in 100 mM NaCl, 10 mM MgCl<sub>2</sub>, and 10 mM Na-cacodylate (pH 7.0).

**Table 2.**  $T_m$  values and thermodynamic data for antiparallel-stranded oligonucleotide duplexes containing **1** and **3** opposite to  $^iG_d$  and  $dG$ .<sup>[a]</sup>

Oligonucleotide duplexes		$T_m$ [°C]	$\Delta H^\circ$ [kcal mol <sup>-1</sup> ]	$\Delta S^\circ$ [cal K <sup>-1</sup> mol <sup>-1</sup> ]	$\Delta G^\circ_{310}$ [kcal mol <sup>-1</sup> ]
5'-d (TAG GTC AAT ACT) 3'-d (ATC CAG TTA TGA)	(ODN-1) (ODN-2)	47	-84	-237	-11.0
5'-d (TAG <b>G</b> TTC AAT ACT) 3'-d (ATC <b>i</b> GAG TTA TGA)	(ODN-1) (ODN-5)	40	-74	-209	-9.1
5'-d (TAG <b>i</b> GTC AAT ACT) 3'-d (ATC <b>G</b> AG TTA TGA)	(ODN-3) (ODN-4)	39	-72	-206	-8.7
5'-d (TAG <b>i</b> GTC AAT ACT) 3'-d (ATC <b>1</b> AG TTA TGA)	(ODN-3) (ODN-6)	42	-74	-210	-9.6
5'-d (TAG <b>i</b> GTC AAT ACT) 3'-d (ATC <b>3</b> AG TTA TGA)	(ODN-3) (ODN-7)	43	-76	-215	-9.7
5'-d (TAG <b>G</b> TTC AAT ACT) 3'-d (ATC <b>G</b> AG TTA TGA)	(ODN-1) (ODN-4)	36	-66	-188	-8.2
5'-d (TAG <b>G</b> TTC AAT ACT) 3'-d (ATC <b>1</b> AG TTA TGA)	(ODN-1) (ODN-6)	30	-62	-178	-7.0
5'-d (TAG <b>G</b> TTC AAT ACT) 3'-d (ATC <b>3</b> AG TTA TGA)	(ODN-1) (ODN-7)	29	-61	-175	-6.7
5'-d (TAG <b>i</b> GTC AAT ACT) 3'-d (ATC <b>i</b> GAG TTA TGA)	(ODN-3) (ODN-5)	34	-64	-183	-7.7

[a] Measured at 260 nm at a single-strand concentration of 5  $\mu$ M + 5  $\mu$ M at a heating rate of 1.0 °C min<sup>-1</sup> in 100 mM NaCl, 10 mM MgCl<sub>2</sub>, and 10 mM Na-codylate (pH 7).  $T_m$  values and thermodynamic data were calculated from the heating curves by using the program Meltwin 3.0.<sup>[18]</sup>

show a significantly higher impact on duplex stability than that of nondendronized 1- $^iG_d$  pairs. The  $\Delta T_m$  value of both base pairs amounts to 5 °C for two incorporations and 9 °C for three incorporations. The stability increase by  $dG$ - $^iG_d$  base pairs is negligible. The stability gain result from two factors: 1) increasing the number of consecutive purine-purine base pairs, and 2) the impact of the dendritic side chain in the case of **3**. Separated incorporation of dendronized 5-aza-7-deazaguanine-isoguanine base pairs shows no  $T_m$  increase. This arrangement reflects the situation (helix distortion at the connecting points) discussed for single incorporations. All other base pair combinations ( $dG$ - $dG$ ,  $^iG_d$ - $dG$ ,  $^iG_d$ - $dC$ ) displayed  $T_m$  values lower than that of the standard duplex. We were surprised by the strong stabilization of the tripropargylamine side chain because we did not expect that three spacious side-chain residues would be so well accommodated in the groove of purine-purine DNA. Thus, one can conclude that the functionalization of a 1- $^iG_d$  base pair with side chains ( $\rightarrow$ 3- $^iG_d$ ) is well accepted by the purine-purine double helix.

### Global helical changes of hybrid DNA induced by 5-aza-7-deazaguanine-isoguanine and guanine-isoguanine base pairs

CD spectroscopy is commonly used to detect global changes on the DNA double helix. A-, B-, and Z-DNA can be clearly distinguished by this technique.<sup>[19]</sup> Herein, the method is used to detect global changes of hybrid DNAs formed by purine-purine and purine-pyrimidine base pairs. In this regard, we performed three types of experiments: 1) CD spectra of hybrid DNA were measured, in which the number of purine-purine base pairs was raised from one to three (Figure 3); 2) CD spec-

tra of duplexes were calculated from single-strand spectra and compared with experimental spectra (Figure 4); and 3) temperature-dependent CD spectra were measured (Figure 5).

Figure 3a-c displays the spectra of 12-mer oligonucleotide duplexes with one, two, and three purine-purine pairs, respectively, aligned in a consecutive way and flanked by Watson-Crick base pairs. Significant differences for the shapes of the CD spectra are observed for all combinations of purine-purine base pairs ( $dG$ - $^iG_d$ , 1- $^iG_d$ , 3- $^iG_d$ ), if the number of incorporations is increased from one to three. In the case of three incorporations, the shape of a Watson-Crick-type B-DNA with a positive lobe at 280 nm and a negative lobe at 245 nm is significantly altered for all base pairs. However, these changes are different for the particular base pairs. The long-wavelength part of the spectra are affected by the long UV wavelength maximum of  $^iG_d$  residues at 292 nm,<sup>[20]</sup> whereas canonical nucleosides show maxima in the region of 260 nm with shoulders at around 280 nm. Therefore,  $^iG_d$  can be used as a sensor for environmental changes. Actually, the duplex with three incorporations of the 1- $^iG_d$  pair shows a positive lobe at about 305 nm (Figure 3b), whereas with three consecutive guanine-isoguanine pairs, the positive lobe is shifted to around 295 nm (Figure 3a). This wavelength shift indicates differences in the type of base pairing between the  $^iG_d$ - $dG$  and 1- $^iG_d$  pairs. One possible explanation is a tautomeric shift required for the formation of a tridentate guanine-isoguanine base pair (NH-1 to NH-3),<sup>[3,4a,b]</sup> which is not required for the tridentate 5-aza-7-deazaguanine-isoguanine base pair. This is associated with a consumption of energy that might also be responsible for the lower stability of the guanine-isoguanine pair (Tables 2 and 3). Another explanation is the lack of nitrogen-7 in 5-aza-7-deazaguanine. In the case of guanine base pairs, nitrogen-7 is pro-

**Table 3.**  $T_m$  values and thermodynamic data of antiparallel-stranded oligonucleotide duplexes containing multiple consecutive and separated incorporations of **1** and **3** opposite to  ${}^iG_d$ .<sup>[a]</sup>

Oligonucleotide duplex		$T_m$ [°C]	$\Delta H^\circ$ [kcal mol <sup>-1</sup> ]	$\Delta S^\circ$ [cal K <sup>-1</sup> mol <sup>-1</sup> ]	$\Delta G^\circ_{310}$ [kcal mol <sup>-1</sup> ]
5'-d (TAG GTC AAT ACT)	(ODN-1)	47	-84	-237	-11.0
3'-d (ATC CAG TTA TGA)	(ODN-2)				
5'-d (TA <sup>i</sup> G <sup>i</sup> GTC AAT ACT)	(ODN-8)	36	-66	-188	-8.2
3'-d (AT G GAG TTA TGA)	(ODN-9)				
5'-d (TA <sup>i</sup> G <sup>i</sup> GTC AAT ACT)	(ODN-8)	46	-81	-229	-10.6
3'-d (AT <b>1</b> AG TTA TGA)	(ODN-10)				
5'-d (TA <sup>i</sup> G <sup>i</sup> GTC AAT ACT)	(ODN-8)	51	-87	-242	-12.2
3'-d (AT <b>3</b> AG TTA TGA)	(ODN-11)				
5'-d (TAG GTC AAT ACT)	(ODN-1)	28	-60	-174	-6.5
3'-d (ATG GAG TTA TGA)	(ODN-9)				
5'-d (TA <sup>i</sup> G <sup>i</sup> GTC AAT ACT)	(ODN-8)	32	-63	-182	-7.4
3'-d (AT <b>C</b> CAG TTA TGA)	(ODN-2)				
5'-d (TAG GT <sup>i</sup> G <sup>i</sup> AAT A <sup>i</sup> GT)	(ODN-12)	33	-63	-180	-7.7
3'-d (ATC CA G TTA T GA)	(ODN-2)				
5'-d (TAG GT <sup>i</sup> G <sup>i</sup> AAT A <sup>i</sup> GT)	(ODN-12)	40	-74	-210	-9.2
3'-d (ATC CA <b>1</b> TTA T <b>1A</b> )	(ODN-13)				
5'-d (TAG GT <sup>i</sup> G <sup>i</sup> AAT A <sup>i</sup> GT)	(ODN-12)	40	-73	-205	-9.1
3'-d (ATC CA <b>3</b> TTA T <b>3A</b> )	(ODN-14)				
5'-d (TAG GTG GGT ACT)	(ODN-16)	54	-88	-243	-13.0
3'-d (ATC CAC CCA TGA)	(ODN-20)				
5'-d (TAG GT <sup>i</sup> G <sup>i</sup> G <sup>i</sup> GT ACT)	(ODN-15)	37	-67	-189	-8.4
3'-d (ATC CA G G GA TGA)	(ODN-17)				
5'-d (TAG GT <sup>i</sup> G <sup>i</sup> G <sup>i</sup> GT ACT)	(ODN-15)	59	-89	-242	-14.4
3'-d (ATC CA <b>1 1 1A</b> TGA)	(ODN-18)				
5'-d (TAG GT <sup>i</sup> G <sup>i</sup> G <sup>i</sup> GT ACT)	(ODN-15)	68	-96	-255	-17.0
3'-d (ATC CA <b>3 3 3A</b> TGA)	(ODN-19)				
5'-d (TAG GTG GGT ACT)	(ODN-16)	39	-71	-202	-8.6
3'-d (ATC CAG GGA TGA)	(ODN-17)				
5'-d (TAG GT <sup>i</sup> G <sup>i</sup> G <sup>i</sup> GT ACT)	(ODN-15)	no	-	-	-
3'-d (ATC CA <b>C C CA</b> TGA)	(ODN-20)	$T_m$			

[a] Measured at 260 nm at a concentration of 5  $\mu$ M + 5  $\mu$ M single strand at a heating rate of 1.0 °C min<sup>-1</sup> in 100 mM NaCl, 10 mM MgCl<sub>2</sub>, and 10 mM Na-codylate (pH 7.0).  $T_m$  values and thermodynamic data were calculated from the heating curves by using the program Meltwin 3.0.<sup>[18]</sup>

truding into the DNA groove and binds water molecules or cations. This is not possible for the 5-aza-7-deazaguanine–isoguanine base pairs, which might affect the global helix structure.

Also, in the case of 7-triopargylamine-5-aza-7-deazaguanine–isoguanine base pairs, a significant change to the CD spectra is observed, if the number of base pairs is increased from one to three (Figure 3c). For three incorporations, the shape of the CD spectrum in the “isoguanine region” at around 300 nm is similar to that with three 5-aza-7-deazaguanine–isoguanine base pairs. Therefore, similar base-pairing properties can be considered. However, a new strongly negative lobe at around 280 nm appears, indicating changes in the global helical structure different from the duplexes containing runs of dG– ${}^iG_d$  or 1– ${}^iG_d$  base pairs.

We anticipate that the triopargylamine side chains protruding into the major groove of the hybrid duplex are responsible for these helical changes.

As discussed, helical changes and the electronic properties of monomeric building blocks are responsible for CD spectral changes. To gain a deeper insight into particular CD changes, spectra of complementary single strands were measured separately and absorbance data were combined to give calculated duplex spectra. Then, the calculated duplex spectra were compared with those experimentally measured. Figure 4a displays the spectra for three incorporations of 5-aza-7-deazaguanine–isoguanine base pairs in the ODN-15-ODN-18 duplex, and Figure 4b for three incorporations of triopargylamine derivative **3**.

All experiments indicate that the measured CD spectra are rather different from those calculated. From Figure 4a and b, it can be seen that the positive lobe at 295 nm of the single strand containing isoguanine is shifted to 305 nm in the duplex. Environmental changes in close proximity to the isoguanine residues are responsible for this shift. The stacked  ${}^iG_d$  residues (single strand) are now involved in base pairing (duplex formation). Furthermore, the strong impact of the tri-

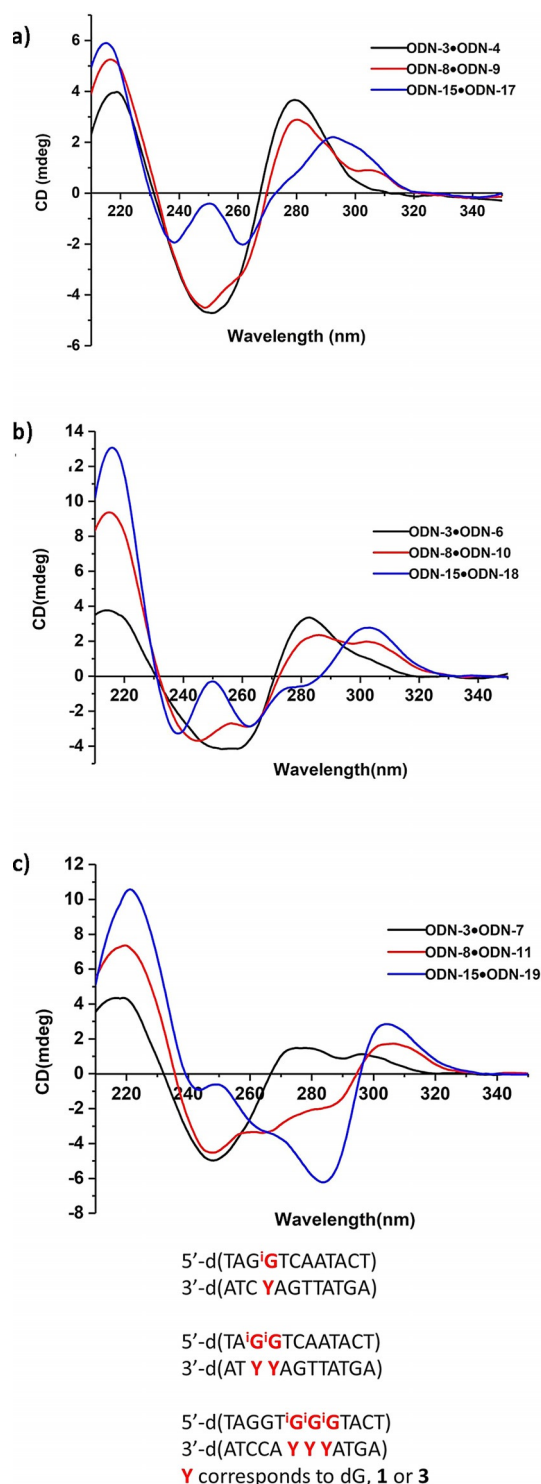


**Figure 3.** CD spectra of oligonucleotide duplexes. Y corresponds to a) dG, b) 1, and c) 3. All measurements were performed with 5  $\mu$ M + 5  $\mu$ M single-strand concentration in 100 mM NaCl, 10 mM MgCl<sub>2</sub>, and 10 mM Na-cacodylate (pH 7.0). The cell path length of the cuvette used to record the CD spectra was 5 mm.

propargyl side chains on the duplex structure becomes apparent. Single-stranded ODN-19 shows only small CD amplitudes, whereas the ODN-15-ODN-19 duplex develops strong CD adsorption.

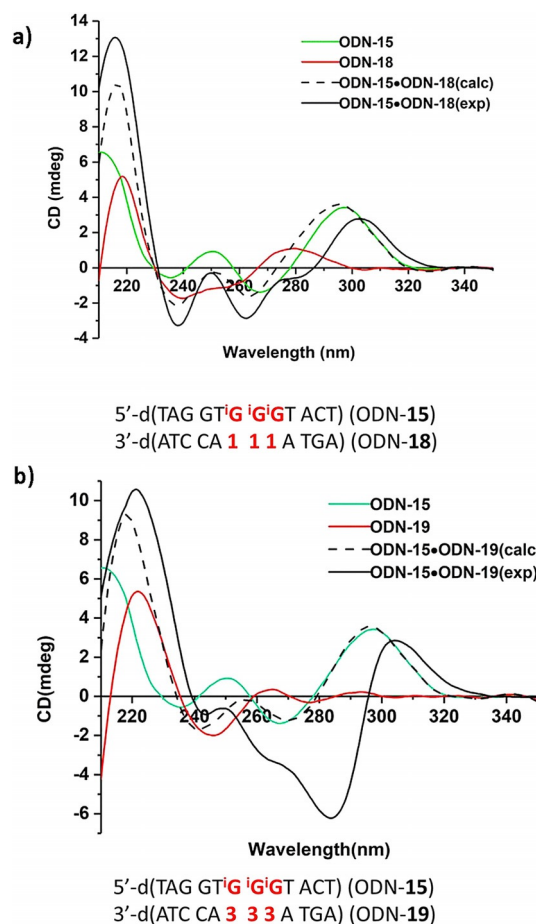


**Figure 4.** CD spectra of a) ODN-15, ODN-18, ODN-15-ODN-18 duplex, and the calculated CD spectrum of ODN-15-ODN-18 duplex (sum of the CD spectra of ODN-15 and ODN-18); b) ODN-15, ODN-19, ODN-15-ODN-19 duplex, and the calculated CD spectrum of ODN-15-ODN-19 duplex (sum of the CD spectra of ODN-15 and ODN-19). All measurements were performed in 100 mM NaCl, 10 mM MgCl<sub>2</sub>, and 10 mM Na-cacodylate, pH 7.0. The cell path length of the cuvette for the CD spectra was 5 mm.

Helical changes are also visible from CD spectra recorded during thermal strand separation (melting). Such information is not available from UV-melting profiles. From Figure 5, it can be clearly seen that changes in CD spectra during melting are similar in the region around 300 nm for both duplexes, but differ significantly in the region from 240 to 290 nm.  $T_m$  values obtained from temperature-dependent CD spectra were the same as those observed from UV-melting profiles.

### Double click functionalization of dendronized 5-aza-7-deazaguanine oligonucleotides with pyrene azide

The tripropargylamine residue allows the simultaneous functionalization of two terminal triple bonds with azides. The monofunctionalized compound is not observed if two equivalents of azide are used. The reaction was already performed on monomeric 5-aza-7-deazaguanine (**3**  $\rightarrow$  **18**; Scheme S1 in the Supporting Information) and on related compounds.<sup>[11c, 12b, d, e, 16fg]</sup> The double click reaction was studied on ODN-7. The reaction is efficient because the dendronized side chain can



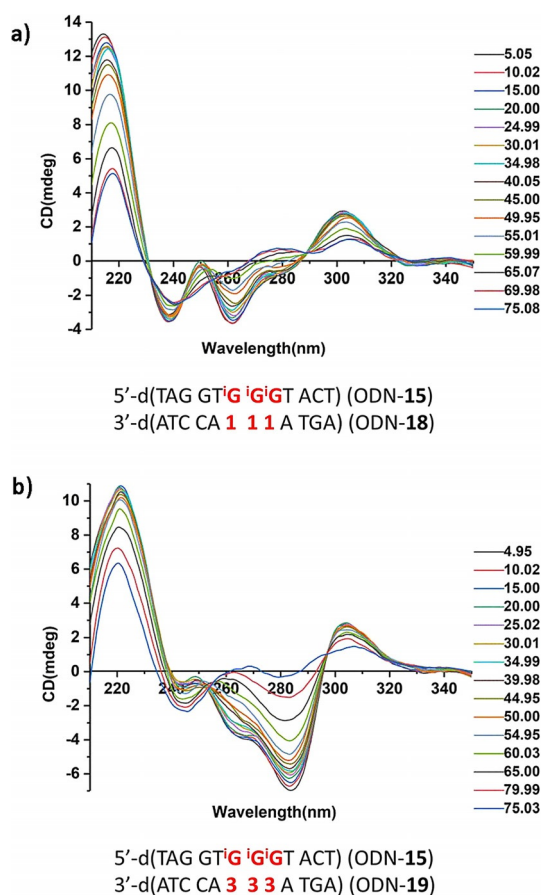
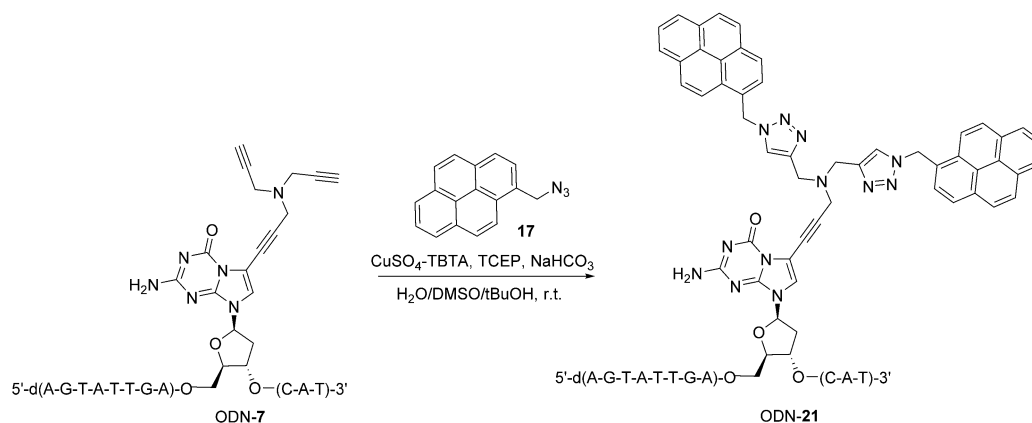


**Figure 5.** Temperature-dependent CD-spectra of a) ODN-15-ODN-18 and b) ODN-15-ODN-19. All measurements were performed in 100 mM NaCl, 10 mM MgCl<sub>2</sub>, and 10 mM Na-cacodylate, pH 7.0. The cell path length of the cuvette for the CD spectra was 5 mm.

complex copper ions, which then develops self-catalytic activity for the click reaction.<sup>[11c]</sup> This reaction represents the first example of side-chain functionalization of a purine-purine base pair by click chemistry. Functionalization proceeds at a position (C-7) accepting spacious residues in purine-purine DNA. Pyrene azide **17** was chosen for this purpose.



**Scheme 2.** Click functionalization of dendronized ODN-7 containing **3** with 1-azidomethylpyrene (**17**).

Pyrene displays attractive properties, if it is connected to oligonucleotides. It acts as a microenvironment-sensitive label and shows monomer and excimer fluorescence.<sup>[16]</sup> Furthermore, pyrene residues are able to intercalate between nucleic acid base pairs and can contribute stability to the helix.<sup>[21]</sup> Herein, the impact of dendrimeric pyrene residues is investigated for 5-aza-7-deazaguanine-isoguanine base pairs embedded in a Watson-Crick double helix. To this end, ODN-7 was chosen as the corresponding duplex ODN-3-ODN-7 containing a single 7-tripropargylamine-5-aza-7-deazaguanine-isoguanine base pair is labile (Table 2). We anticipated that duplex stability would be restored, if one or two of the dendritic pyrene residues were present that could stabilize DNA. Due to the large surface area of purine-purine base pairs, pyrene intercalation and stacking with purine bases in the duplex might overcome helix deformation at the connection points.

The Huisgen-Meldal-Sharpless cycloaddition click functionalization<sup>[22]</sup> was performed with ODN-7 by using tris(carboxyethyl)phosphine (TCEP) instead of ascorbic acid for the reduction of copper (II) to copper(I) and tris(benzyltriazolylmethyl)amine (TBTA) to complex the copper ions. Excess **17** was used with respect to one oligonucleotide molecule (Scheme 2). The reaction conditions followed a partly modified protocol recently published by our laboratory (for details, see the Experimental Section).<sup>[16f,g]</sup> The reaction succeeded and bis-click product ODN-21 was formed at RT within 12 h. Due to the lipophilicity of the pyrene moieties, the functionalized oligonucleotide showed a significantly longer retention time by HPLC than that of the precursor oligonucleotide (Figure S3 in the Supporting Information). Characterization and purity of the clicked oligonucleotide was validated by HPLC and MALDI-TOF spectra.

Then, the photophysical properties of the 7-tripropargylamine pyrene conjugate in a single-stranded oligonucleotide and an oligonucleotide duplex were studied. Identical concentrations in aqueous buffer were used. In a previous study, we observed that the double-clicked pyrene 5-aza-7-deazaguanosine monomer showed excimer emission ( $\approx 470$  nm) and monomer emission ( $\approx 395$  nm).<sup>[11c]</sup> Compared with that, the fluorescence of the pyrene-functionalized single strand (ODN-21) and the ODN-3-ODN-21 duplex did not exhibit excimer emis-

sion (Figure 6a), supporting that pyrene residues develop strong stacking interactions with proximal base pairs. Nevertheless, the fluorescence intensity of the duplex is less than that for single-stranded ODN-21. Because pyrene is sensitive to environmental changes, fluorescence is quenched more strongly in the duplex environment than that of single strands.

Next, the pyrene-functionalized oligonucleotide was hybridized with the complementary strand (ODN-3) containing isoguanine opposite to the pyrene conjugate.  $T_m$  values for these duplexes were measured and compared with the nonclicked precursor ODN-3-ODN-7 duplex (Table 4). Compared with non-

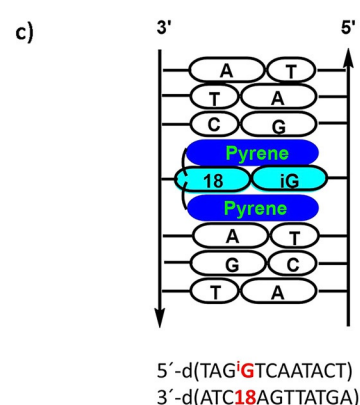
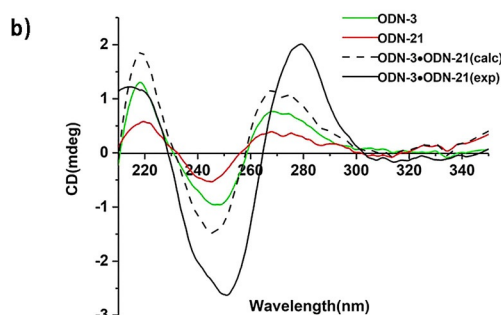
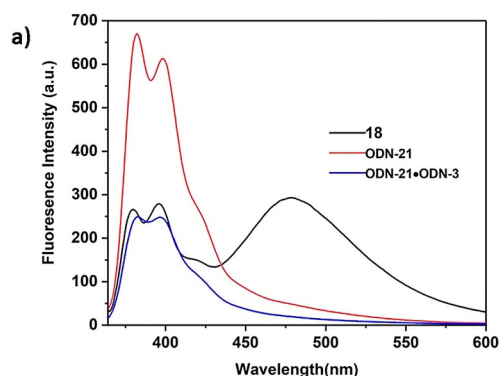
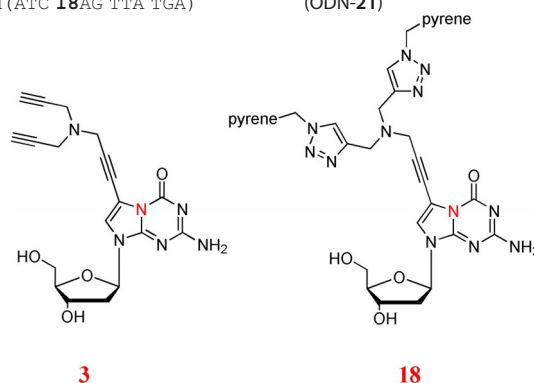


**Figure 6.** a) Fluorescence emission spectra of pyrene click conjugate **18** (black, 5  $\mu$ M), ODN-21 (red, 2  $\mu$ M), and ODN-3-ODN-21 duplex (blue, 2  $\mu$ M of each strand). All spectra were measured in 100 mM NaCl, 10 mM MgCl<sub>2</sub>, and 10 mM Na-cacodylate (pH 7.0). b) CD spectra of ODN-3, ODN-21, ODN-3-ODN-21 duplex, and the calculated CD spectrum of ODN-3-ODN-21 duplex (sum of the CD spectra of ODN-3 and ODN-21). c) Pyrene intercalation in a Watson-Crick duplex incorporating one **18**-iG<sub>d</sub> purine-purine base pair.

**Table 4.**  $T_m$  values of oligonucleotide duplexes containing tripropargylated **3** and the pyrene click adduct **4**.<sup>[a]</sup>

Duplex	$T_m$ [°C]
5'-d (TAG <b>G</b> TC AAT ACT) (ODN-1)	47
3'-d (ATC <b>C</b> AG TTA TGA) (ODN-2)	
5'-d (TAG <sup>i</sup> <b>G</b> TC AAT ACT) (ODN-3)	43
3'-d (ATC <b>3</b> AG TTA TGA) (ODN-7)	
5'-d (TAG <sup>i</sup> <b>G</b> TC AAT ACT) (ODN-3)	54
3'-d (ATC <b>18</b> AG TTA TGA) (ODN-21)	



[a] Measured at 260 nm at a concentration of 5  $\mu$ M + 5  $\mu$ M single strand at a heating rate of 1.0 °C min<sup>-1</sup> in 100 mM NaCl, 10 mM MgCl<sub>2</sub>, and 10 mM Na-cacodylate (pH 7.0).  $T_m$  values were calculated from the heating curves by using the program Meltwin 3.0.<sup>[18]</sup>

clicked tripropargylamine precursor **3**, pyrene click conjugate **18** opposite to iG<sub>d</sub> induces strong duplex stabilization (Table 4). This duplex is even more stable than that with a dG-dC base pair in the same position ( $\Delta T_m = +7$  °C). Stabilization of pyrene by intercalation in Watson-Crick duplexes, including interaction opposite to abasic sites, is reported in the literature by various laboratories.<sup>[12d,e,16b,f,21]</sup> However, this work is the first example of purine-purine DNA being stabilized by pyrene.

To visualize the impact of the pyrene residues on the double-helix structure, CD spectra were measured (Figure 6b). In more detail, measurements were performed on ODN-3 and ODN-21 single strands and the ODN-3-ODN-21 duplex and compared with calculated values obtained by the addition of CD spectra of single strands. A positive lobe at about 285 nm and a negative lobe at about 245 nm are observed. The shape of the curve is similar to that of the reference ODN-1-ODN-2 duplex, but different to the ODN-3-ODN-7 duplex, containing one tripropargylated 3-iG<sub>d</sub> base pair.

Taken together, the following observations were made on the pyrene-functionalized duplex containing purine-purine pairs: 1) fluorescence quenching of the pyrene residues in the double strand compared with the single strand, 2) strong duplex stabilization by the **18**-iG<sub>d</sub> base pair, 3) the CD spectrum of the ODN-3-ODN-21 duplex has the typical shape of a B-DNA, and 4) loss of excimer fluorescence in oligonucleotides. Thus, we propose that both pyrene residues are intercalated between the 5-aza-7-deazaguanine-isoguanine pair and the proximal Watson-Crick base pairs (Figure 6c). Apparently, the modified pyrene nucleoside residue acts as a bis-intercalator,<sup>[23]</sup> thereby stabilizing the duplex through  $\pi$ - $\pi$  stacking interac-

tions with neighboring Watson–Crick base pairs. As a result, pyrene is able to compensate for the negative impact caused by a single  ${}^iG_d$ -3 purine–purine pair in a Watson–Crick duplex.

## Conclusion

This work reported on hybrid DNAs with Watson–Crick and purine–purine base pairs in the double helix. To this end, oligonucleotides were synthesized with single and multiple incorporations of **1**, **3**, and  ${}^iG_d$ . After hybridization, DNA was formed with base pairs of guanine, 5-aza-7-deazaguanine, and dendronized 7-triopargylamine-5-aza-7-deazaguanine opposite isoguanine. Upon embedding in the Watson–Crick DNA, changes to DNA stability and helix structure were monitored. More specifically, 1) duplex stability of Watson–Crick DNA decreased if a single purine–purine base pair was inserted in place of a canonical base pair; 2) functionalization of the dendritic triopargylamine side chain with two pyrene residues increased duplex stability, and thus, the linker length between the two pyrene residues was sufficient to place both pyrene residues in the double helix next to the 5-aza-7-deazaguanine–isoguanine base pair acting as a bis-intercalator; 3) duplex stability strongly increased with a growing number of 5-aza-7-deazaguanine–isoguanine base pairs, thereby forming purine–purine tracts; 4) stabilization was particularly strong if triopargylamine side chains were present; and 5) on the contrary, duplexes with  $dG$ - ${}^iG_d$  base pairs showed low  $T_m$  values and no positive change upon increasing the number of base pairs incorporated (Figure 7).

Global changes to the DNA double-helix structure were monitored by CD spectra. Significant differences in the shape of the spectra were observed for all combinations of  $dG$ - ${}^iG_d$ ,  $1$ - ${}^iG_d$ , and  $3$ - ${}^iG_d$  base pairs, if the number of incorporations was increased from one to three. For three incorporations, the typical spectral shape of a Watson–Crick-type B-DNA (positive

lobe at 280 nm, negative lobe at 245 nm) was significantly altered for all base pairs. Calculated duplex spectra obtained from those of single strands and experimentally measured duplexes differed significantly, indicating global changes of the hybrid DNA helix structure in solution with respect to the Watson–Crick DNA.

The successful functionalization of 5-aza-7-deazaguanine–isoguanine base pairs and the positive impact of the side chains showed that spacious residues introduced in the 7-position of **1** were well accommodated in the large groove of purine–purine DNA. This study opens the way for new applications in DNA chemistry, chemical biology, and materials science,<sup>[24]</sup> as well as for the storage of genetic and nongenetic information in the DNA molecule.<sup>[9e,25]</sup> It steps into new areas of molecular recognition by purine bases with complementary hydrogen bonds, but not complementary in size and different to canonical DNA.

## Experimental Section

**General:** All chemicals and solvents were of laboratory grade, as obtained from commercial suppliers, and were used without further purification. Reversed-phase HPLC was carried out by using a Hitachi 655A-12 intelligent pump and a 655A variable-wavelength UV monitor connected to an integrator on a  $4 \times 250$  mm RP-18 (10  $\mu$ m) LiChrospher 100 column. The molecular masses of the oligonucleotides were determined by means of MALDI-TOF MS on a Bruker Autoflex Speed spectrometer in linear positive mode with 3-hydroxypicolinic acid (3-HPA) as a matrix. The thermal melting curves were measured with an Agilent Technologies Cary 100 Bio UV/Vis spectrophotometer equipped with a thermoelectrical controller. The temperature was measured continuously in the reference cell with a Pt-100 resistor at a heating rate of  $1^\circ\text{C min}^{-1}$ .  $T_m$  values were determined from the melting curves by using the software Meltwin, version 3.0.<sup>[18]</sup> CD spectra were recorded at  $25^\circ\text{C}$  on a Jasco J-815 spectrometer.

**Oligonucleotide syntheses and characterization:** Solid-phase oligonucleotide syntheses were performed on an ABI 392-08 synthesizer at 1  $\mu$ mol scale (trityl-on mode) by employing the phosphoramidites of **1**,<sup>[7]</sup> **3**, and  ${}^iG_d$ ,<sup>[17]</sup> as well as the standard building blocks with an average coupling yield over 95%. After cleavage from the solid support, the oligonucleotides were deprotected in 28% aqueous ammonia at  $55^\circ\text{C}$  for 2 h. The DMT-containing oligonucleotides were purified by reversed-phase HPLC (RP-18) with the gradient system at 260 nm: A) MeCN, B) 0.1 M  $(\text{Et}_3\text{NH})\text{OAc}$  (pH 7.0)/MeCN, 95:5; gradient I: 0–3 min 10–15% A in B, 3–15 min 15–50% A in B; flow rate 0.7  $\text{mL min}^{-1}$ . The purified “trityl-on” oligonucleotides were treated with 2.5%  $\text{CHCl}_2\text{COOH}/\text{CH}_2\text{Cl}_2$  for 2 min at  $0^\circ\text{C}$  to remove the 4,4'-dimethoxytrityl residues. The detritylated oligomers were purified again by reversed-phase HPLC with gradient II: 0–20 min 0–20% A in B; 20–25 min, 20% A in B; flow rate 0.7  $\text{mL min}^{-1}$ . The oligonucleotides were desalted on a reversed-phase column (RP-18) by using water for elution of salt, whereas the oligonucleotides were eluted with  $\text{H}_2\text{O}/\text{CH}_3\text{OH}$  (2:3). The oligonucleotides were lyophilized on a Speed-Vac evaporator to yield colorless solids, which were frozen at  $-24^\circ\text{C}$ . The purity of all oligonucleotides was confirmed by means of RP-18 HPLC (Figure S3 in the Supporting Information) and MALDI-TOF MS (Table 1). The extinction coefficients,  $\epsilon_{260}$  ( $\text{H}_2\text{O}$ ), of the nucleosides are as follows: dA, 15 400; dG, 11 700; dT, 8800; dC, 7300;  $z^2G_d$ , 14 100;<sup>[26]</sup>  ${}^iG_d$ , 4300  $\text{dm mol}^{-1} \text{cm}^{-1}$ .<sup>[27]</sup> The extinction coefficients of the oligonu-

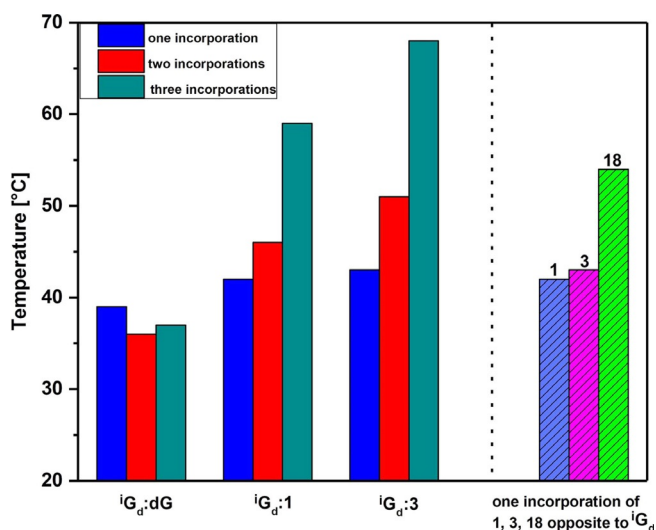


**Figure 7.** Left: Bar diagram comparing  $T_m$  values for one, two, and three incorporations of  $dG$ - ${}^iG_d$ ,  $dG$ ,  $1$ - ${}^iG_d$ , and  $3$ - ${}^iG_d$  base pairs in a Watson–Crick duplex. Right: A comparison of the  $T_m$  values for one incorporation of  $1$ - ${}^iG_d$ ,  $3$ - ${}^iG_d$ , and  $18$ - ${}^iG_d$  base pairs in a Watson–Crick duplex.

cleotides were calculated from the sum of the extinction coefficients of nucleoside constituents by considering the hypochromic change for particular single strands.

**Anomeric mixture of 2-amino-8-[2-deoxy- $\beta$ -D-erythro-pentofuranosyl]-6-iodo-8H-imidazo[1,2-a]-s-triazin-4-one (6) and 2-amino-8-[2-deoxy- $\alpha$ -D-erythro-pentofuranosyl]-6-iodo-8H-imidazo[1,2-a]-s-triazin-4-one (7):** Compound **6** (2.0 g, 5.76 mmol) was dissolved in MeCN (200 mL) under gentle warming, then  $K_2CO_3$  (2.54 g, 18.43 mmol) and TDA-1 (0.25 mL, 0.15 mmol) were added under stirring. Stirring was continued at RT for 15 min. Then, 2-deoxy-3,5-di-O-toluoyl- $\alpha$ -D-erythro-pentofuranosyl chloride (**5**)<sup>[28]</sup> (3.58 g, 9.22 mmol) was added and stirring was continued for 1.5 h. The mixture was filtered, the filtrate was evaporated, and the remaining residue was applied to flash chromatography (FC; silica gel, column 12×4 cm,  $CH_2Cl_2/MeOH$  98:2). From the main zone, an anomeric mixture of the protected compounds was obtained as a colorless solid (2.7 g, 70%). The solid was suspended in  $NH_3/MeOH$  (100 mL) and stirred at RT overnight. The solvent was evaporated and the remaining residue was purified by FC (silica gel, column 10×4 cm,  $CH_2Cl_2/MeOH$ , 95:5→85:15). From the main zone, an anomeric mixture of **6** and **7** was obtained as a colorless solid (1.3 g, 86%).  $^1H$  NMR (600 MHz,  $[D_6]DMSO$ , 26 °C):  $\delta$  = 2.09 (dt,  $J$  = 2.3, 14.5 Hz, 1H;  $C2'_{\alpha}$ -H<sub>α</sub>), 2.14 (ddd,  $J$  = 3.2, 6.0, 13.2 Hz, 1H;  $C2'_{\beta}$ -H<sub>β</sub>), 2.35 (ddd,  $J$  = 5.7, 7.7, 13.2 Hz, 1H;  $C2'_{\beta}$ -H<sub>β</sub>), 2.64 (ddd,  $J$  = 6.4, 8.0, 14.4 Hz, 1H;  $C2'_{\alpha}$ -H<sub>α</sub>), 3.39 (t,  $J$  = 5.1 Hz, 1H;  $C5'$ -H<sub>α</sub>), 3.47–3.56 (m, 2H;  $C5'$ -H<sub>β</sub>), 3.78 (td,  $J$  = 2.6, 4.3 Hz, 1H;  $C4'$ -H<sub>β</sub>), 4.10 (td,  $J$  = 2.2, 4.5 Hz, 1H;  $C4'$ -H<sub>α</sub>), 4.25–4.31 (m, 2H;  $C3'$ -H<sub>α,β</sub>), 4.84 (t,  $J$  = 5.6 Hz, 1H;  $C5'$ -OH<sub>α</sub>), 4.97 (t,  $J$  = 5.4 Hz, 1H;  $C5'$ -OH<sub>β</sub>), 5.27 (d,  $J$  = 3.9 Hz, 1H;  $C3'$ -OH<sub>β</sub>), 5.49 (d,  $J$  = 3.4 Hz, 1H;  $C3'$ -OH<sub>α</sub>), 6.11–6.16 (m, 2H;  $C1'$ -H<sub>α,β</sub>), 6.92 (d,  $J$  = 31.4 Hz, 4H;  $2 \times NH_2$  α<sub>β</sub>), 7.57 (s, 1H; C8-H<sub>β</sub>), 7.60 ppm (s, 1H; C8-H<sub>α</sub>);  $^{13}C$  NMR (151 MHz,  $[D_6]DMSO$ , 26 °C):  $\delta$  = 56.8 (C-7<sub>α</sub>), 57.5 (C-7<sub>β</sub>), 61.4 (C-5'<sub>β</sub>), 61.6 (C-5'<sub>α</sub>), 70.3 (C-3'<sub>β</sub>), 70.5 (C-3'<sub>α</sub>), 82.8 (C-1'<sub>β</sub>), 83.7 (C-1'<sub>α</sub>), 87.6 (C-4'<sub>β</sub>), 89.0 (C-4'<sub>α</sub>), 121.0 (C-8<sub>β</sub>), 122.1 (C-8<sub>α</sub>), 150.1 (C-4<sub>β</sub>), 150.2 (C-4<sub>α</sub>), 150.3 (C-2<sub>α</sub>), 150.5 (C-2<sub>β</sub>), 164.2 (C-6<sub>α</sub>), 164.2 ppm (C-6<sub>β</sub>); UV/Vis (MeOH):  $\lambda_{max}$  ( $\epsilon$ ) = 267 nm ( $15500 \text{ mol}^{-1} \text{ dm}^3 \text{ cm}^{-1}$ ); HRMS (ESI-TOF):  $m/z$  calcd for  $C_{10}H_{12}I_2N_3NaO_4^+$  [ $M + Na$ ]<sup>+</sup>: 415.9832; found: 415.9824.

**Separation of the anomeric mixture of 6 and 7 by 4,4'-dimethoxytritylation:** The anomeric mixture of **6** and **7** (1.0 g, 2.55 mmol) was dried by repeated coevaporation with dry pyridine (3×20 mL) and suspended in dry pyridine (30 mL). Then, DMT-Cl (1.21 g, 3.56 mmol) was added, and the mixture was stirred for 3 h at RT. Then, the mixture was diluted with  $CH_2Cl_2$  (200 mL) and a 5% aqueous solution of  $NaHCO_3$  (200 mL) was added. The organic phase was dried over  $Na_2SO_4$  and evaporated, and the residue was separated by FC (silica gel, column 10×4 cm,  $CH_2Cl_2/MeOH$ , 96:4).

**2-Amino-8-[2-deoxy-5-O-(4,4'-dimethoxytriphenylmethyl)- $\beta$ -D-erythro-pentofuranosyl]-6-iodo-8H-imidazo[1,2-a]-s-triazin-4-one (8):** From the slower migrating zone, compound **8** was obtained as a colorless foam (660 mg, 37%). Analytical data were identical to those reported earlier.<sup>[11b]</sup> TLC (silica gel,  $CH_2Cl_2/MeOH$ , 95:5):  $R_f$  = 0.3;  $^1H$  NMR (600 MHz,  $[D_6]DMSO$ , 26 °C):  $\delta$  = 2.22 (ddd,  $J$  = 13.4, 6.4, 4.7 Hz, 1H;  $C2'$ -H<sub>α</sub>), 3.12 (ddd,  $J$  = 13.6, 10.4, 4.5 Hz, 2H;  $2 \times C5'$ -H), 3.74 (s, 6H;  $2 \times OCH_3$ ), 3.89 (dt,  $J$  = 5.7, 3.8 Hz, 1H;  $C4'$ -H), 4.34 (td,  $J$  = 9.0, 4.5 Hz, 1H;  $C3'$ -H), 5.33 (d,  $J$  = 4.5 Hz, 1H;  $C3'$ -OH), 6.14 (t,  $J$  = 6.4 Hz, 1H;  $C1'$ -H), 6.87 (dd,  $J$  = 9.0, 3.1 Hz, 4H; Ar-H), 6.99 (d,  $J$  = 5.1 Hz, 2H;  $NH_2$ ), 7.25–7.15 (m, 5H; Ar-H), 7.29 (t,  $J$  = 7.7 Hz, 2H; Ar-H), 7.36 (dd,  $J$  = 8.4, 1.2 Hz, 2H; Ar-H), 7.42 ppm (s, 1H; C7-H);  $^{13}C$  NMR (151 MHz,  $[D_6]DMSO$ , 26 °C):  $\delta$  = 38.6 (C-2'), 55.0 ( $OCH_3$ ), 57.7 (C-7), 63.8 (C-5'), 70.0 (C-3'), 82.7 (C-1'), 85.5 (C-4'), 85.7, 113.1 (Ar-C), 120.8 (C-8), 126.6 (Ar-C), 127.6 (Ar-C), 127.8 (Ar-C), 129.6 (Ar-C), 129.6 (Ar-C), 135.4 (Ar-C), 135.5 (Ar-C), 144.8 (Ar-C), 150.1 (C-2), 150.6 (C-4), 158.0 (Ar-C), 164.2 ppm (C=O); UV/Vis (MeOH):  $\lambda_{max}$

( $\epsilon$ ) = 267 nm ( $16500 \text{ mol}^{-1} \text{ dm}^3 \text{ cm}^{-1}$ ); HRMS (ESI-TOF):  $m/z$  calcd for  $C_{31}H_{30}IN_3NaO_6^+$  [ $M + Na$ ]<sup>+</sup>: 718.1138; found: 718.1136.

**2-Amino-8-[2-deoxy-5-O-(4,4'-dimethoxytriphenylmethyl)- $\alpha$ -D-erythro-pentofuranosyl]-6-iodo-8H-imidazo[1,2-a]-s-triazin-4-one (9):** From the faster migrating zone, compound **9** was obtained as a colorless foam (560 mg, 31%). Analytical data were identical to those reported earlier.<sup>[11b]</sup> TLC (silica gel,  $CH_2Cl_2/MeOH$ , 95:5):  $R_f$  = 0.4;  $^1H$  NMR (600 MHz,  $[D_6]DMSO$ , 26 °C):  $\delta$  = 2.20–2.13 (m, 1H;  $C2'$ -H<sub>β</sub>), 2.71–2.63 (m, 1H;  $C2'$ -H<sub>α</sub>), 2.97 (dd,  $J$  = 10.2, 4.6 Hz, 1H;  $C5'$ -H), 3.09 (dd,  $J$  = 10.2, 4.0 Hz, 1H;  $C5'$ -H), 3.74 (s, 6H;  $2 \times OCH_3$ ), 4.30–4.21 (m, 2H;  $C3'$ -H,  $C4'$ -H), 3.74 (s, 6H;  $2 \times OCH_3$ ), 5.56 (d,  $J$  = 3.4 Hz, 1H;  $C3'$ -OH), 6.21 (dd,  $J$  = 7.8, 2.5 Hz, 1H;  $C1'$ -H), 6.90 (m, 5H; Ar-H,  $NH_2$ ), 7.25–7.21 (m, 5H; Ar-H), 7.35–7.30 (m, 2H; Ar-H), 7.37 (dd,  $J$  = 8.4, 1.2 Hz, 2H; Ar-H), 7.63 ppm (s, 1H; C7-H);  $^{13}C$  NMR (151 MHz,  $[D_6]DMSO$ , 26 °C):  $\delta$  = 40.0 (C-2'), 55.0 ( $OCH_3$ ), 56.9 (C-7), 63.8 (C-5'), 70.9 (C-3'), 83.9 (C-1'), 85.6 (quat. C), 87.1 (C-4'), 113.2 (Ar-C), 122.1 (C-8), 126.7 (Ar-C), 127.6 (Ar-C), 127.9 (Ar-C), 129.6 (Ar-C), 135.4 (Ar-C), 135.4 (Ar-C), 144.7 (Ar-C), 150.2 (C-2), 150.3 (C-4), 158.0 (arom. C), 164.2 ppm (C=O); UV/Vis (MeOH):  $\lambda_{max}$  ( $\epsilon$ ) = 267 nm ( $16900 \text{ mol}^{-1} \text{ dm}^3 \text{ cm}^{-1}$ ); HRMS (ESI-TOF):  $m/z$  calcd for  $C_{31}H_{30}IN_3NaO_6^+$  [ $M + Na$ ]<sup>+</sup>: 718.1138; found: 718.1136.

**2-[(Dibutylamino)methylidene]amino-8-(2-deoxy-5-O-(4,4'-dimethoxytriphenylmethyl)- $\beta$ -D-erythro-pentofuranosyl)-6-iodo-8H-imidazo[1,2-a]-s-triazin-4-one (10):** Dibutylformamide dimethyl acetal (100  $\mu$ L) was added to a suspension of **8** (71 mg, 0.1 mmol) in MeOH (5 mL). The mixture was stirred at 40 °C for 1 h (TLC monitoring) and then the solvent was evaporated. The residue was applied to FC (silica gel, column 10×3 cm,  $CH_2Cl_2/MeOH$ , 95:5) to give **10** (69 mg, 83%). TLC (silica gel,  $CH_2Cl_2/MeOH$ , 95:5):  $R_f$  = 0.5;  $^1H$  NMR (600 MHz,  $[D_6]DMSO$ , 26 °C):  $\delta$  = 0.91 (d,  $J$  = 3.3 Hz, 6H;  $2 \times CH_3$ ), 1.20–1.35 (m, 4H;  $2 \times CH_2$ ), 1.55 (dddd,  $J$  = 14.8, 9.5, 7.0, 4.7 Hz, 4H;  $2 \times CH_2$ ), 2.27 (ddd,  $J$  = 13.5, 6.7, 4.8 Hz, 1H;  $C2'$ -H<sub>α</sub>), 3.11 (dd,  $J$  = 10.4, 3.2 Hz, 1H;  $C2'$ -H<sub>β</sub>), 3.16–3.22 (m, 2H;  $C5'$ -H), 3.39–3.50 (m, 4H;  $2 \times CH_2$ ), 3.73 (d,  $J$  = 1.3 Hz, 6H;  $2 \times OCH_3$ ), 3.91 (ddd,  $J$  = 6.0, 4.3, 3.1 Hz, 1H;  $C4'$ -H), 4.36 (dq,  $J$  = 6.4, 4.7 Hz, 1H;  $C3'$ -H), 5.36 (d,  $J$  = 4.8 Hz, 1H;  $C3'$ -OH), 6.29 (t,  $J$  = 6.3 Hz, 1H;  $C1'$ -H), 6.84–6.88 (m, 5H; Ar-H), 7.19–7.26 (m, 6H; Ar-H), 7.28 (dd,  $J$  = 8.5, 7.0 Hz, 2H; Ar-H), 7.36 (dd,  $J$  = 8.5, 1.3 Hz, 2H; Ar-H), 7.56 (s, 1H; C8-H), 8.71 ppm (s, 1H; NCH);  $^{13}C$  NMR (151 MHz,  $[D_6]DMSO$ , 26 °C):  $\delta$  = 13.5 ( $CH_3$ ), 13.7 ( $CH_3$ ), 19.1 ( $CH_2$ ), 19.6 ( $CH_2$ ), 28.6 ( $CH_2$ ), 30.4 ( $CH_2$ ), 44.9 ( $NCH_2$ ), 51.2 ( $NCH_2$ ), 55.0 ( $OCH_3$ ), 58.1 (C-7), 63.8 (C-5'), 64.9, 70.0 (C-3'), 82.8 (C-1'), 85.5 (quat. C), 85.8 (C-4'), 113.1 (Ar-C), 123.2 (Ar-C), 126.6 (Ar-C), 127.6 (Ar-C), 129.6 (Ar-C), 135.5 (Ar-C), 144.8 (Ar-C), 150.4 (C-2), 150.6 (C-4), 158.0 (Ar-C), 159.5 (N=CH), 168.6 ppm (C=O); UV/Vis (MeOH):  $\lambda_{max}$  ( $\epsilon$ ) = 311 (26300), 276 nm ( $18300 \text{ mol}^{-1} \text{ dm}^3 \text{ cm}^{-1}$ ); HRMS (ESI-TOF)  $m/z$  calcd for  $C_{40}H_{47}IN_6NaO_6$  [ $M + Na$ ]<sup>+</sup>: 857.2499; found: 857.2505.

**2-[(Dibutylamino)methylidene]amino-8-(2-deoxy-5-O-(4,4'-dimethoxytriphenylmethyl)- $\alpha$ -D-erythro-pentofuranosyl)-6-iodo-8H-imidazo[1,2-a]-s-triazin-4-one (11):** Dibutylformamide dimethyl acetal (100  $\mu$ L) was added to a suspension of **9** (200 mg, 0.29 mmol) in MeOH (5 mL). The mixture was stirred at 40 °C for 1 h (TLC monitoring) and then the solvent was evaporated. The residue was applied to FC (silica gel, column 10×3 cm,  $CH_2Cl_2/MeOH$ , 95:5) to give **11** (189 mg, 79%). TLC (silica gel,  $CH_2Cl_2/MeOH$ , 95:5):  $R_f$  = 0.5;  $^1H$  NMR (600 MHz,  $[D_6]DMSO$ , 26 °C):  $\delta$  = 0.88 (dt,  $J$  = 14.5, 7.4 Hz, 6H;  $2 \times CH_3$ ), 1.19–1.33 (m, 4H;  $2 \times CH_2$ ), 1.53 (dddd,  $J$  = 16.8, 12.6, 8.7, 6.7 Hz, 4H;  $2 \times CH_2$ ), 2.19 (dt,  $J$  = 14.3, 2.8 Hz, 1H;  $C2'$ -H<sub>α</sub>), 2.70 (ddd,  $J$  = 14.2, 8.0, 6.8 Hz, 1H;  $C2'$ -H<sub>β</sub>), 2.98 (dd,  $J$  = 10.2, 4.8 Hz, 1H;  $C5'$ -H), 3.07–3.12 (m, 1H;  $C5'$ -H), 3.15–3.23 (m, 2H;  $CH_2$ ), 3.46 (td,  $J$  = 7.3, 3.6 Hz, 2H;  $CH_2$ ), 3.73 (d,  $J$  = 0.8 Hz, 6H;  $2 \times OCH_3$ ), 4.27 (ddt,  $J$  = 12.0, 6.4, 3.0 Hz, 2H; C-3'-H,  $C4'$ -H), 5.62 (d,  $J$  = 3.7 Hz, 1H;  $C3'$ -OH), 6.37 (dd,  $J$  = 7.7, 3.0 Hz, 1H;  $C1'$ -H),

6.91 (dd,  $J=9.1$ , 2.5 Hz, 4H; Ar-H), 7.20–7.28 (m, 5H; Ar-H), 7.33 (dd,  $J=8.4$ , 7.1 Hz, 2H; Ar-H), 7.37–7.42 (m, 2H; Ar-H), 7.77 (s, 1H; H-8), 8.70 ppm (s, 1H; NCH);  $^{13}\text{C}$  NMR (151 MHz,  $[\text{D}_6]\text{DMSO}$ , 26 °C):  $\delta=13.5$  ( $\text{CH}_3$ ), 13.7 ( $\text{CH}_3$ ), 19.1 ( $\text{CH}_2$ ), 19.6 ( $\text{CH}_2$ ), 28.6 ( $\text{CH}_2$ ), 30.4 ( $\text{CH}_2$ ), 44.7 ( $\text{NCH}_2$ ), 51.1 ( $\text{NCH}_2$ ), 55.0 ( $\text{OCH}_3$ ), 57.5 (C-7), 63.8 (C-5'), 70.8 (C-3'), 84.2 (C-1'), 85.6 (quat. C), 87.1 (C-4'), 113.2 (Ar-C), 122.0 (Ar-C), 123.2 (C-8), 126.6 (Ar-C), 127.6 (Ar-C), 129.69 (Ar-C), 135.4 (Ar-C), 144.8 (Ar-C), 150.4 (C-2), 150.5 (C-4), 158.0 (Ar-C), 159.6 (N=CH), 162.5 (Ar-C), 168.6 ppm (C=O); UV/Vis (MeOH):  $\lambda_{\text{max}}$  ( $\epsilon$ ) = 311 (26500), 277 nm ( $19600 \text{ mol}^{-1} \text{ dm}^3 \text{ cm}^{-1}$ ); HRMS (ESI-TOF):  $m/z$  calcd for  $\text{C}_{31}\text{H}_{30}\text{IN}_5\text{O}_6\text{H}$  [ $M+H$ ] $^+$ : 857.2499; found: 857.2494.

**2-[[Dibutylamino)methylidene]amino]-8-(2-deoxy-5-O-(4,4'-dimethoxytriphenylmethyl)- $\beta$ -D-erythro-pentofuranosyl)-6-iodo-8H-imidazo[1,2-a]-s-triazin-4-one 3'-(2-cyanoethyl diisopropylphosphoramidite) (12):** 2-Cyanoethyl diisopropylphosphoramidochloridite (40  $\mu\text{L}$ , 0.18 mmol) was added at RT to a solution of compound **10** (100 mg, 0.12 mmol) and anhydrous  $i\text{Pr}_2\text{EtN}$  (36  $\mu\text{L}$ , 0.20 mmol) in anhydrous  $\text{CH}_2\text{Cl}_2$  (5 mL). After stirring for 5 min, TLC monitoring showed the formation of faster migrating compound **12**, but it decomposed immediately. TLC (silica gel,  $\text{CH}_2\text{Cl}_2$ /acetone, 80:20):  $R_f=0.4$ .

**2-[[Dibutylamino)methylidene]amino]-8-(2-deoxy-5-O-(4,4'-dimethoxytriphenylmethyl)- $\alpha$ -D-erythro-pentofuranosyl)-6-iodo-8H-imidazo[1,2-a]-s-triazin-4-one 3'-(2-cyanoethyl diisopropylphosphoramidite) (13):** 2-Cyanoethyl diisopropylphosphoramidochloridite (40  $\mu\text{L}$ , 0.18 mmol) was added at RT to a solution of compound **11** (100 mg, 0.12 mmol) and anhydrous  $i\text{Pr}_2\text{EtN}$  (36  $\mu\text{L}$ , 0.20 mmol) in anhydrous  $\text{CH}_2\text{Cl}_2$  (5 mL). After stirring for 5 min, TLC monitoring showed the formation of faster migrating compound **13**, but it decomposed immediately. TLC (silica gel,  $\text{CH}_2\text{Cl}_2$ /acetone, 80:20):  $R_f=0.4$ .

**2-Amino-8-(2-deoxy-5-O-(4,4'-dimethoxytriphenylmethyl)- $\beta$ -D-erythro-pentofuranosyl)-6-[3-(di(prop-2-yn-1-yl)amino)prop-1-yn-1-yl]-8H-imidazo[1,2-a]-s-triazin-4-one (14):** [ $\text{Pd}(\text{PPh}_3)_4$ ] (30 mg, 0.025 mmol, 0.1 equiv),  $\text{Et}_3\text{N}$  (69  $\mu\text{L}$ , 0.50 mmol, 2 equiv),  $\text{CuI}$  (10 mg, 0.050 mmol, 0.2 equiv), and tripropargylamine (360  $\mu\text{L}$ , 2.50 mmol, 10 equiv) were added to a suspension of nucleoside **8** (0.25 mmol, 1 equiv) in DMF (2 mL) in an oven-dried round-bottomed flask. The reaction mixture was stirred at RT under  $\text{N}_2$  for 6 h. Purification by FC (silica gel, column 15  $\times$  2 cm,  $\text{CH}_2\text{Cl}_2$ /MeOH, 87:13) and evaporation of the main zone gave compound **14** (69 mg 69%) as a colorless foam. TLC (silica gel,  $\text{CH}_2\text{Cl}_2$ /MeOH, 9:1):  $R_f=0.4$ ;  $^1\text{H}$  NMR (600 MHz,  $[\text{D}_6]\text{DMSO}$ , 26 °C):  $\delta=2.25$  (ddd,  $J=5.2$ , 6.6, 13.6 Hz, 1H; C2'-H $_{\alpha}$ ), 2.51–2.53 (m, 1H; C2'-H $_{\beta}$ ), 3.08–3.12 (m, 2H; 2  $\times$  C5'-H), 3.12–3.17 (m, 1H), 3.23 (t,  $J=2.4$  Hz, 2H; 2  $\times$  C $\equiv$ H), 3.45 (d,  $J=2.5$  Hz, 4H; 2  $\times$  CH $_2$ ), 3.61 (d,  $J=1.3$  Hz, 2H; CH $_2$ ), 3.73 (d,  $J=1.7$  Hz, 7H; 2  $\times$  OCH $_3$ ), 3.86–3.91 (m, 1H; C4'-H), 4.36 (p,  $J=5.1$  Hz, 1H; C3'-H), 5.37 (d,  $J=4.5$  Hz, 1H; C3'-OH), 6.15 (t,  $J=6.1$  Hz, 1H; C1'-H), 6.84 (dd,  $J=1.7$ , 9.0 Hz, 4H; Ar-H), 7.05 (s, 2H; NH $_2$ ), 7.20–7.23 (m, 5H; Ar-H), 7.27 (t,  $J=7.7$  Hz, 2H; Ar-H), 7.32–7.37 (m, 3H; Ar-H), 7.65 ppm (s, 1H; C8-H);  $^{13}\text{C}$  NMR (151 MHz,  $[\text{D}_6]\text{DMSO}$ , 26 °C):  $\delta=38.6$  (C-2'), 41.2 (CH $_2$ ), 42.0 (CH $_2$ ), 55.0 (OCH $_3$ ), 63.8 (C-5'), 69.8 (C-3'), 72.8 (C), 76.0 (C), 79.1 (C), 82.8 (C-1'), 85.5 (C-4'), 85.7 (qC), 91.0 (C), 105.0 (C-7), 113.2 (Ar-C), 119.5 (Ar-C), 126.7 (Ar-C), 127.7 (Ar-C), 127.8 (Ar-C), 129.7 (Ar-C), 129.7 (Ar-C), 135.4 (Ar-C), 135.6 (Ar-C), 144.9 (Ar-C), 149.8 (C-2), 150.2 (C-4), 158.1, 165.1 ppm (C=O); UV/Vis (MeOH):  $\lambda_{\text{max}}$  ( $\epsilon$ ) = 265 nm ( $19300 \text{ mol}^{-1} \text{ dm}^3 \text{ cm}^{-1}$ ); HRMS (ESI-TOF):  $m/z$  calcd for  $\text{C}_{40}\text{H}_{39}\text{N}_6\text{O}_6$  [ $M+H$ ] $^+$ : 699.2931; found: 699.2973.

**2-[[Dibutylamino)methylidene]amino]-8-(2-deoxy-5-O-(4,4'-dimethoxytriphenylmethyl)- $\beta$ -D-erythro-pentofuranosyl)-6-[3-(di(prop-2-yn-1-yl)amino)prop-1-yn-1-yl]-8H-imidazo[1,2-a]-s-triazin-4-one (15):** *N,N*-Dibutylformamide dimethyl acetal (627 mg,

2.90 mmol) was added under stirring to a suspension of compound **14** (225 mg, 0.322 mmol) in MeOH (15 mL). Stirring was continued for 4 h at 50 °C. Then, the solvent was evaporated and the remaining residue was submitted to FC (silica gel, column 10  $\times$  2 cm, EtOAc/acetone, 95:5). From the main zone, compound **15** was obtained as a colorless foam (176 mg, 65%). TLC (silica gel, EtOAc/acetone, 90:10):  $R_f=0.3$ ;  $^1\text{H}$  NMR (600 MHz,  $[\text{D}_6]\text{DMSO}$ , 26 °C):  $\delta=0.91$  (td,  $J=3.4$ , 7.4 Hz, 6H; 2  $\times$  CH $_3$ ), 1.29 (ddq,  $J=7.4$ , 14.7, 20.2 Hz, 4H; 2  $\times$  CH $_2$ ), 1.52–1.60 (m, 4H; 2  $\times$  CH $_2$ ), 2.30 (ddd,  $J=5.5$ , 6.8, 13.5 Hz, 1H; H $_{\alpha}$ -2'), 2.51–2.55 (m, 1H; H $_{\beta}$ -2'), 3.12 (dd,  $J=3.2$ , 10.4 Hz, 1H; H $_{\alpha}$ -5'), 3.20 (dd,  $J=6.1$ , 10.4 Hz, 1H; H $_{\beta}$ -5'), 3.24 (t,  $J=2.4$  Hz, 2H; 2  $\times$  C $\equiv$ H), 3.42 (t,  $J=7.2$  Hz, 2H; CH $_2$ ), 3.45–3.50 (m, 6H; 3  $\times$  CH $_2$ ), 3.63 (d,  $J=1.4$  Hz, 2H; CH $_2$ ), 3.73 (d,  $J=2.6$  Hz, 6H; 2  $\times$  OCH $_3$ ), 3.91 (ddd,  $J=3.2$ , 4.8, 6.1 Hz, 1H; C4'-H), 4.37 (p,  $J=5.3$  Hz, 1H; C3'-H), 5.37 (d,  $J=4.9$  Hz, 1H; C3'-OH), 6.30 (dd,  $J=5.4$ , 6.7 Hz, 1H; C1'-H), 6.82–6.86 (m, 4H; Ar-H), 7.19–7.24 (m, 5H; Ar-H), 7.25–7.29 (m, 2H; Ar-H), 7.33–7.37 (m, 2H; Ar-H), 7.79 (s, 1H; C8-H), 8.72 ppm (s, 1H, N=CH);  $^{13}\text{C}$  NMR (151 MHz,  $[\text{D}_6]\text{DMSO}$ , 26 °C):  $\delta=13.5$  (CH $_3$ ), 13.7 (CH $_3$ ), 19.1 (CH $_2$ ), 19.6 (CH $_2$ ), 28.6 (CH $_2$ ), 30.4 (CH $_2$ ), 38.8 (C-2'), 40.0, 41.1 (CH $_2$ ), 42.0 (CH $_2$ ), 44.8 (CH $_2$ ), 51.2 (CH $_2$ ), 55.0 (OCH $_3$ ), 63.7 (C-5'), 69.7 (C-3'), 72.6 (C), 75.9 (C), 79.0 (C), 82.9 (C-1'), 85.5 (C-4'), 85.7 (quat. C), 91.3 (C), 105.0 (C-7), 113.1 (Ar-C), 120.5 (C-8), 126.6 (Ar-C), 127.6 (Ar-C), 127.8 (Ar-C), 129.6 (Ar-C), 129.7 (Ar-C), 135.3 (Ar-C), 135.5 (Ar-C), 144.8 (Ar-C), 149.9 (C-2), 150.0 (C-4), 158.0, 159.6 (N=CH), 169.5 ppm (C=O); UV/Vis (MeOH):  $\lambda_{\text{max}}$  ( $\epsilon$ ) = 312 (32300), 266 (28100), 234 nm ( $28800 \text{ mol}^{-1} \text{ dm}^3 \text{ cm}^{-1}$ ); HRMS (ESI-TOF):  $m/z$  calcd for  $\text{C}_{49}\text{H}_{56}\text{N}_7\text{O}_6$  [ $M+H$ ] $^+$ : 838.4292; found: 838.4318.

**2-[[Dibutylamino)methylidene]amino]-8-(2-deoxy-5-O-(4,4'-dimethoxytriphenylmethyl)- $\beta$ -D-erythro-pentofuranosyl)-6-[3-(di(prop-2-yn-1-yl)amino)prop-1-yn-1-yl]-8H-imidazo[1,2-a]-s-triazin-4-one 3'-(2-cyanoethyl diisopropylphosphoramidite) (16):** 2-Cyanoethyl diisopropylphosphoramidochloridite (14  $\mu\text{L}$ , 0.081 mmol) was added at RT to a solution of compound **15** (40 mg, 0.048 mmol) and anhydrous  $i\text{Pr}_2\text{EtN}$  (16  $\mu\text{L}$ , 0.072 mmol) in anhydrous  $\text{CH}_2\text{Cl}_2$  (2.5 mL). After stirring for 20 min, the mixture was diluted with  $\text{CH}_2\text{Cl}_2$  (5 mL) and the reaction was quenched by adding a 5% aqueous solution of  $\text{NaHCO}_3$  (10 mL). Then, the aqueous layer was extracted with  $\text{CH}_2\text{Cl}_2$  (60 mL) and the combined organic layer was dried ( $\text{Na}_2\text{SO}_4$ ) and evaporated. The residual colorless oil was applied to FC (silica gel, column 10  $\times$  2 cm,  $\text{CH}_2\text{Cl}_2$ /acetone, 9:1). From the main zone, a colorless foam of compound **16** was obtained as a mixture of diastereoisomers (30 mg, 65%). TLC (silica gel,  $\text{CH}_2\text{Cl}_2$ /acetone, 80:20):  $R_f=0.4$ ;  $^{31}\text{P}$  NMR (121 MHz,  $\text{CDCl}_3$ ):  $\delta=148.83$ , 148.89 ppm; HRMS (ESI-TOF):  $m/z$  calcd for  $\text{C}_{58}\text{H}_{73}\text{N}_9\text{O}_7\text{P}$  [ $M+H$ ] $^+$ : 1038.5371; found: 1038.5364.

**General procedure for Huisgen–Meldal–Sharpless [3+2] cycloaddition:**  $\text{CuSO}_4\cdot\text{TETA}$  (1:2) ligand complex (50  $\mu\text{L}$  of a 20 mM stock solution in  $\text{H}_2\text{O}/\text{DMSO}/t\text{BuOH}$ , 4:3:1), TCEP (50  $\mu\text{L}$  of a 20 mM stock solution in water),  $\text{NaHCO}_3$  (50  $\mu\text{L}$ , 200 mM stock solution in water), **17** (100  $\mu\text{L}$  of a 20 mM stock solution in  $\text{H}_2\text{O}/\text{dioxane}/\text{DMSO}$ , 1:1:1), and DMSO (30  $\mu\text{L}$ ) were added to a single-stranded oligonucleotide (5  $A_{260}$  units), and the reaction mixture was stirred at room temperature for 12 h. The reaction mixture was concentrated under vacuum and dissolved in double-distilled water (500  $\mu\text{L}$ ) and centrifuged for 30 min at 14000 rpm. The supernatant solution was collected and further purified by reversed-phase HPLC with the gradient 0–3 min 10–15% B in A, 3–15 min 15–50% B in A, 15–20 min 50–10% B in A; flow rate 0.7  $\text{cm}^3 \text{ min}^{-1}$ . The molecular masses of the oligonucleotides were determined by MALDI-TOF MS.

## Acknowledgements

We thank Dr. Simone Budow-Busse for critical reading of the manuscript. We would like to thank Dr. Letzel, Organisch-Chemisches Institut, Universität Münster, Germany, for the measurement of the mass spectra and Prof. Dr. B. Wunsch, Institut für Pharmazeutische und Medizinische Chemie, Universität Münster, for provide us with access to a 600 MHz NMR spectrometer. We appreciate Xenia Jentgens for the synthesis of oligonucleotides. Open access funding enabled and organized by Projekt DEAL.

## Conflict of interest

The authors declare no conflict of interest.

**Keywords:** DNA · molecular recognition · nucleosides · oligonucleotides · purine–purine base pairing

- [1] a) J. D. Watson, F. H. C. Crick, *Nature* **1953**, *171*, 737–738; b) F. Seela, X. Peng, H. Li, P. Chittepu, K. I. Shaikh, J. He, Y. He, I. Mikhailopolu, *Collect. Symp. Ser.* **2005**, *7*, 1–20.
- [2] F. Seela, C. Wei, *Helv. Chim. Acta* **1999**, *82*, 726–745.
- [3] J. Hunziker, H.-J. Roth, M. Böhringer, A. Giger, U. Diederichsen, M. Göbel, R. Krishnan, B. Jaun, C. Leumann, A. Eschenmoser, *Helv. Chim. Acta* **1993**, *76*, 259–352.
- [4] a) T. R. Battersby, M. Albalos, M. J. Friesenhahn, *Chem. Biol.* **2007**, *14*, 525–531; b) B. D. Heuberger, C. Switzer, *ChemBioChem* **2008**, *9*, 2779–2783.
- [5] a) H. Liu, J. Gao, S. R. Lynch, Y. D. Saito, L. Maynard, E. T. Kool, *Science* **2003**, *302*, 868–871; b) H. Liu, J. Gao, E. T. Kool, *J. Am. Chem. Soc.* **2005**, *127*, 1396–1402; c) N. J. Leonard, *Acc. Chem. Res.* **1982**, *15*, 128–135.
- [6] a) S. Hoshika, I. Singh, C. Switzer, R. W. Molt Jr., N. A. Leal, M.-J. Kim, M.-S. Kim, H.-J. Kim, M. M. Georgiadis, S. A. Benner, *J. Am. Chem. Soc.* **2018**, *140*, 11655–11660; b) J. V. Skelly, K. J. Edwards, T. C. Jenkins, S. Neidle, *Proc. Natl. Acad. Sci. USA* **1993**, *90*, 804–808; c) F. V. Murphy IV, V. Ramakrishnan, *Nat. Struct. Mol. Biol.* **2004**, *11*, 1251–1252; d) P. W. R. Corfield, W. N. Hunter, T. Brown, P. Robinson, O. Kennard, *Nucleic Acids Res.* **1987**, *15*, 7935–7949.
- [7] F. Seela, S. Amberg, A. Melenevski, H. Rosemeyer, *Helv. Chim. Acta* **2001**, *84*, 1996–2014.
- [8] H. Rosemeyer, F. Seela, *J. Org. Chem.* **1987**, *52*, 5136–5143.
- [9] a) F. Seela, A. Melenevski, *Eur. J. Org. Chem.* **1999**, 485–496; b) F. Seela, A. Melenevski, C. Wei, *Bioorg. Med. Chem. Lett.* **1997**, *7*, 2173–2176; c) F. Seela, H. Rosemeyer in *Recent Advances in Nucleosides: Chemistry and Chemotherapy* (Ed.: C. K. Chu), Elsevier Science B. V., Amsterdam, **2002**, pp. 505–533; d) S. Hoshika, N. A. Leal, M.-J. Kim, M.-S. Kim, N. B. Karalkar, H.-J. Kim, A. M. Bates, N. E. Watkins Jr., H. A. SantaLucia, A. J. Meyer, S. DasGupta, J. A. Piccirilli, A. D. Ellington, J. SantaLucia Jr., M. M. Georgiadis, S. A. Benner, *Science* **2019**, *363*, 884–887; e) L. Zhang, Z. Yang, K. Sefah, K. M. Bradley, S. Hoshika, M.-J. Kim, H.-J. Kim, G. Zhu, E. Jiménez, S. Cansiz, I.-T. Teng, C. Champanhac, C. McLendon, C. Liu, W. Zhang, D. L. Gerloff, Z. Huang, W. Tan, S. A. Benner, *J. Am. Chem. Soc.* **2015**, *137*, 6734–6737.
- [10] F. Seela, K. I. Shaikh, *Helv. Chim. Acta* **2006**, *89*, 2794–2814.
- [11] a) W. Lin, X. Zhang, F. Seela, *Helv. Chim. Acta* **2004**, *87*, 2235–2244; b) P. Leonard, D. Kondhare, X. Jentgens, C. Daniliuc, F. Seela, *J. Org. Chem.* **2019**, *84*, 13313–13328; c) D. Kondhare, A. Zhang, P. Leonard, F. Seela, *J. Org. Chem.* **2020**, *85*, 10525–10538.
- [12] a) M. Karskela, M. Helkear, P. Virta, H. Lönnberg, *Bioconjugate Chem.* **2010**, *21*, 748–755; b) H. Xiong, P. Leonard, F. Seela, *Bioconjugate Chem.* **2012**, *23*, 856–870; c) J. Qiu, A. Wilson, A. H. El-Sagheer, T. Brown, *Nucleic Acids Res.* **2016**, *44*, e138; d) V. R. Sirivolu, P. Chittepu, F. Seela, *ChemBioChem* **2008**, *9*, 2305–2316; e) F. Seela, H. Xiong, S. Budow, *Tetrahedron* **2010**, *66*, 3930–3943.
- [13] T. Horn, C.-A. Chang, M. S. Urdea, *Nucleic Acids Res.* **1997**, *25*, 4842–4849.
- [14] a) S. M. Grayson, J. M. J. Fréchet, *Chem. Rev.* **2001**, *101*, 3819–3867; b) C. Ornelas, J. R. Aranzaes, E. Cloutet, S. Alves, D. Astruc, *Angew. Chem. Int. Ed.* **2007**, *46*, 872–877; *Angew. Chem.* **2007**, *119*, 890–895; c) J. A. Johnson, M. G. Finn, J. T. Koberstein, N. J. Turro, *Macromol. Rapid Commun.* **2008**, *29*, 1052–1072; d) A.-M. Caminade, C.-O. Turrin, J.-P. Majoral, *Chem. Eur. J.* **2008**, *14*, 7422–7432; e) R. H. E. Hudson, M. J. Damha, *J. Am. Chem. Soc.* **1993**, *115*, 2119–2124; f) M. Endo, T. Majima, *Chem. Commun.* **2006**, 2329–2331; g) C. R. DeMattei, B. Huang, D. A. Tomalia, *Nano Lett.* **2004**, *4*, 771–777; h) M. S. Schepinov, I. A. Udalova, A. J. Bridgman, E. M. Southern, *Nucleic Acids Res.* **1997**, *25*, 4447–4454.
- [15] T. Horn, M. S. Urdea, *Nucleic Acids Res.* **1989**, *17*, 6959–6967.
- [16] a) F. M. Winnik, *Chem. Rev.* **1993**, *93*, 587–614; b) M. E. Østergaard, P. J. Hrdlicka, *Chem. Soc. Rev.* **2011**, *40*, 5771–5788; c) E. Mayer-Enthart, H.-A. Wagenknecht, *Angew. Chem. Int. Ed.* **2006**, *45*, 3372–3375; *Angew. Chem.* **2006**, *118*, 3451–3453; d) A. Okamoto, K. Tainaka, K.-i. Nishiza, I. Saito, *J. Am. Chem. Soc.* **2005**, *127*, 13128–13129; e) I. V. Astakhova, V. A. Korshun, J. Wengel, *Chem. Eur. J.* **2008**, *14*, 11010–11026; f) F. Seela, S. A. Ingale, *J. Org. Chem.* **2010**, *75*, 284–295; g) S. A. Ingale, S. S. Pujari, V. R. Sirivolu, P. Ding, H. Xiong, H. Mei, F. Seela, *J. Org. Chem.* **2012**, *77*, 188–199; h) P. L. Paris, J. M. Langenhan, E. T. Kool, *Nucleic Acids Res.* **1998**, *26*, 3789–3793; i) H. Mei, S. A. Ingale, F. Seela, *Tetrahedron* **2013**, *69*, 4731–4742; j) U. B. Christensen, E. B. Pedersen, *Helv. Chim. Acta* **2003**, *86*, 2090–2097; k) J. Telser, K. A. Cruickshank, L. E. Morrison, T. L. Netzler, C.-k. Chan, *J. Am. Chem. Soc.* **1989**, *111*, 7226–7232.
- [17] a) C. Roberts, R. Bandaru, C. Switzer, *Tetrahedron Lett.* **1995**, *36*, 3601–3604; b) F. Seela, Y. Chen, A. Melenevski, H. Rosemeyer, C. Wei, *Acta Biochim. Pol.* **1996**, *43*, 45–52.
- [18] J. A. McDowell, D. H. Turner, *Biochemistry* **1996**, *35*, 14077–14089.
- [19] a) J. Kypř, I. Kejnovská, D. Renčuk, M. Vorlíčková, *Nucleic Acids Res.* **2009**, *37*, 1713–1725; b) T. Miyahara, H. Nakatsuji, H. Sugiyama, *J. Phys. Chem. A* **2013**, *117*, 42–55.
- [20] Z. Kazimierczuk, R. Mertens, W. Kawczynski, F. Seela, *Helv. Chim. Acta* **1991**, *74*, 1742–1748.
- [21] a) T. S. Kumar, A. S. Madsen, M. E. Østergaard, J. Wengel, P. J. Hrdlicka, *J. Org. Chem.* **2008**, *73*, 7060–7066; b) S. M. Langenegger, R. Häner, *ChemBioChem* **2005**, *6*, 848–851; c) C. Lou, A. Dallmann, P. Marafini, R. Gao, T. Brown, *Chem. Sci.* **2014**, *5*, 3836–3844; d) U. B. Christensen, E. B. Pedersen, *Nucleic Acids Res.* **2002**, *30*, 4918–4925.
- [22] a) M. Meldal, C. W. Tornøe, *Chem. Rev.* **2008**, *108*, 2952–3015; b) R. Huisgen, *Pure Appl. Chem.* **1989**, *61*, 613–628; c) H. C. Kolb, M. G. Finn, K. B. Sharpless, *Angew. Chem. Int. Ed.* **2001**, *40*, 2004–2021; *Angew. Chem.* **2001**, *113*, 2056–2075.
- [23] a) M. Nakamura, Y. Fukunaga, K. Sasa, Y. Ohtoshi, K. Kanaori, H. Hayashi, H. Nakano, K. Yamana, *Nucleic Acids Res.* **2005**, *33*, 5887–5895; b) D. M. Bassani, J. Wirz, R. Hochstrasser, W. Leupin, *J. Photochem. Photobiol. A* **1996**, *100*, 65–76; c) M. Bahr, V. Gabelica, A. Granzhan, M.-P. Teulade-Fichou, E. Weinhold, *Nucleic Acids Res.* **2008**, *36*, 5000–5012.
- [24] a) M. R. Jones, N. C. Seeman, C. A. Mirkin, *Science* **2015**, *347*, 1260901; b) E. Stulz, G. Clever, M. Shionoya, C. Mao, *Chem. Soc. Rev.* **2011**, *40*, 5633–5635; c) F. Aldaye, A. L. Palmer, H. F. Sleiman, *Science* **2008**, *321*, 1795–1799.
- [25] a) L. C. Meiser, P. L. Antkowiak, J. Koch, W. D. Chen, A. X. Kohli, W. J. Stark, R. Heckel, R. N. Grass, *Nat. Protoc.* **2020**, *15*, 86–101; b) Modified nucleosides, *Biochemistry Biotechnology and Medicine* (Ed.: P. Herdewijn), Wiley-VCH, Weinheim, **2008**.
- [26] X. Zhou, D. Kondhare, P. Leonard, F. Seela, *Chem. Eur. J.* **2019**, *25*, 10408–10419.
- [27] F. Seela, C. Wei, *Helv. Chim. Acta* **1997**, *80*, 73–85.
- [28] M. Hoffer, *Chem. Ber.* **1960**, *93*, 2777–2781.

Manuscript received: December 4, 2020

Accepted manuscript online: January 14, 2021

Version of record online: March 18, 2021